

Pervasive increase in tree mortality across the Australian continent

Received: 27 February 2025

Accepted: 24 November 2025

Published online: 6 January 2026

 Check for updates

A list of authors and their affiliations appears at the end of the paper

Widespread climate-driven increases in background tree mortality rates have the potential to reduce the carbon storage of terrestrial ecosystems, challenging their effectiveness as natural buffers against atmospheric CO₂ enrichment with major consequences for the global carbon budget. However, the global extent of trends in tree mortality and their drivers remains poorly quantified. The Australian continent experiences one of the most variable climates on Earth and is host to a diverse range of forest biomes that have evolved high resistance to disturbance, providing a valuable test case for the pervasiveness of tree mortality trends. Here we compile an 83-year tree dynamics database (1941–2023) from >2,700 forest plots across Australia covering tropical savanna and rainforest and warm and cool temperate forests, to explore spatiotemporal patterns of tree mortality and the associated drivers. Over the past eight decades, we found a consistent trend of increasing tree mortality across the four forest biomes. This temporal trend persisted after accounting for stand structure and was exacerbated in forests with low moisture index or a high competition index. Species with traits associated with high growth rate—low wood density, high specific leaf area and short maximum height—exhibited higher average mortality, but the rate of mortality increase was comparable across different functional groups. Increasing mortality was not associated with increasing growth, given that stand basal area increments either declined or remained unchanged over time, but it was associated with increasing temperature over time. Our findings suggest that ongoing climate change has driven pervasive shifts in forest dynamics beyond natural recovery in a range of forest biomes with high resilience to disturbance, threatening the enduring capacity of forests to sequester carbon under current and future climate scenarios.

Tree mortality is a key demographic process that drives changes in forest structure and shapes the fate of carbon with impacts on the climate system^{1–3}. Background mortality rates in forests are generally low (1–3% per year), but even a slight increase in the annual rate, compounded through time, can markedly alter the pace of forest dynamics over centuries^{4,5}. Monitoring since the 1960s has revealed a concerning long-term rise in background mortality rates across a range of ecosystems worldwide, including tropical rainforests in the Amazon⁶ and

Australia⁷, temperate forests in the western USA^{8,9} and Europe¹⁰, and boreal forests¹¹ in Canada, although African tropical forests showed no significant change¹². This rise in background mortality has been accompanied by more frequent observations of large-scale mortality pulses, with abundant examples of drought and heat-induced mortality events reported in the past three decades^{13,14}. An ongoing increase both in background mortality rates and the number of regional forest mortality events would trigger an acceleration of vegetation turnover¹⁵,

✉ e-mail: rllu@stu.ecnu.edu.cn; b.medlyn@westernsydney.edu.au

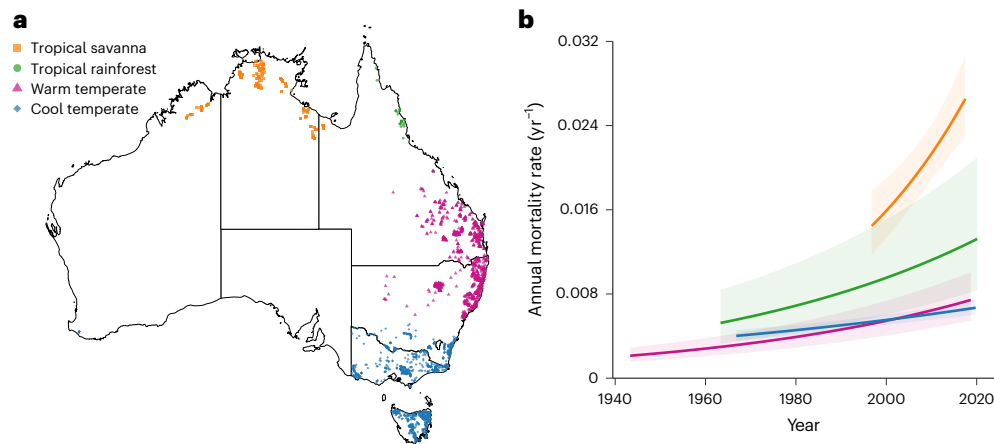


Fig. 1 | Spatial coverage and temporal trajectories of tree mortality across four major forest biomes in Australia. **a**, The geographic distribution of forest plots in four major biomes: tropical savannas (orange), tropical rainforests (green), warm temperate forests (purple) and cool temperate forests (blue). Biome classifications are based on climatic and vegetative criteria (Methods). **b**, Modelled temporal trends in mean annual mortality rates (solid lines) with 95% CIs (shaded areas), accounting for forest structural variation using initial stand basal area for each census, colour-coded by biome as shown in **a**. Temporal

coverage and sample sizes vary by biome: tropical savannas (1994–2018; $n = 198$ plots), tropical rainforests (1963–2023; $n = 25$ plots), warm temperate forests (1941–2023; $n = 1,168$ plots) and cool temperate forests (1965–2023; $n = 1,333$ plots). Although modelled mortality rates increased across all biomes, observed mortality in tropical savannas showed high interannual variability (Extended Data Fig. 1), probably due to shorter monitoring duration and plot turnover (Extended Data Fig. 2). Mortality trends in this biome should therefore be interpreted with caution.

potentially constraining the carbon sink of global forests^{16,17}. However, the global extent of these patterns and their underlying drivers remain poorly understood¹⁸, and tree mortality rates are one of the key uncertainties in future projections of the carbon sink^{19,20}.

The Australian continent provides a valuable test case for evaluating the generality of long-term trends in tree mortality. Wide gradients in temperature and precipitation foster a rich diversity of forest ecosystems across the continent, from tropical savannas and rainforests to cool temperate moist forests²¹. In addition, the Australian climate is characterized by high natural variability, compounded by periodic disturbances such as droughts, floods, heatwaves, wildfires and cyclones²². Many tree species have evolved specialized strategies to survive disturbance, including high stem embolism resistance^{23,24}, deep roots to access soil moisture and groundwater during prolonged drought^{25,26}, and the capacity for epicormic and basal resprouting^{27,28}. Understanding the demographic responses of Australian forests therefore provides critical insight into the vulnerability of Earth's forests under climate change. Global satellite-derived vegetation indices indicate that, although escalating water stress has led to a general decline in vegetation resilience across most tropical and temperate forests, Australian forests exhibit an unexpected trend of increasing resilience²⁹. Similarly, regional simulations from land surface models show no apparent increase in physiological stress or drought-induced mortality in southeastern Australia under a warming and drying climate³⁰. However, this broad-scale evidence of resilience contrasts with emerging ground-based observations. For example, citizen science initiatives such as the Dead Tree Detective project³¹ have documented extensive forest dieback and tree mortality events across Australia during the 2017–2019 drought, suggesting that even historically resilient forests are approaching their physiological limits under the accelerating pace of climate change. These divergent response patterns across scales underscore key gaps in our understanding of species-specific mortality dynamics, especially when mortality is gradual rather than catastrophic³². In this respect, long-term and temporally consistent tree monitoring provides a foundation for identifying the drivers of mortality and its recent dynamics, thereby improving projections of vegetation trajectories and their carbon-cycle consequences under current and future climate change¹⁸.

Here, we conduct a continent-scale assessment of temporal variation in tree mortality leveraging up to 83 years of tree records from 2,724 plots distributed throughout the forested area of Australia (Supplementary Tables 1–3). Our dataset comprised 203,721 individual trees from 958 species, with 26,227 documented tree deaths. The plots were classified into four major biomes based on climate zones and dominant vegetation types: tropical savanna, tropical rainforest, warm temperate forest and cool temperate forest (Fig. 1a; Methods). We developed a suite of generalized linear mixed-effects models to quantify long-term mortality trends and evaluate the drivers across biomes. Because many of our forest plots have experienced historical disturbances such as wildfires or logging and are currently in a phase of recovery through secondary succession, stand basal area was included as a covariate in all mortality models to account for potential confounding effects of forest structural changes on the residual temporal trends. To examine which factors mediated average mortality rates and the pace of temporal changes in mortality rates, we then built models that captured mortality dynamics at multiple biological scales, considering variations in plot mean climate, species functional traits, individual tree size and their interactions through time. To identify the proximate climatic drivers of mortality, we examined the effects of drought quantified using the minimum standardized precipitation–evapotranspiration index ($SPEI_{min}$), maximum temperature (T_{max}) and vapour pressure deficit (VPD). Finally, to test whether observed mortality trends were linked to changes in forest growth dynamics, we analysed temporal trends in tree-level diameter growth and stand-level basal area increment.

Temporal trends and drivers of tree mortality

We found a general increase in tree mortality rates over time in all four forest biomes (Fig. 1). The overall temporal trend, quantified as the annual fractional change in mortality rate, was most pronounced in tropical savannas at 0.032 yr^{-1} from 1994 to 2018 (95% confidence interval (CI) 0.018–0.046) (Supplementary Methods 1). This was followed by increases of 0.019 yr^{-1} in warm temperate forests (95% CI 0.016–0.022, 1941–2023), 0.018 yr^{-1} in tropical rainforests (95% CI 0.015–0.021, 1963–2023) and 0.01 yr^{-1} in cool temperate forests (95% CI 0.007–0.014, 1965–2023). Overall, mean background mortality rates were highest in tropical savannas ($0.03 \pm 0.04 \text{ yr}^{-1}$, mean \pm s.d.),

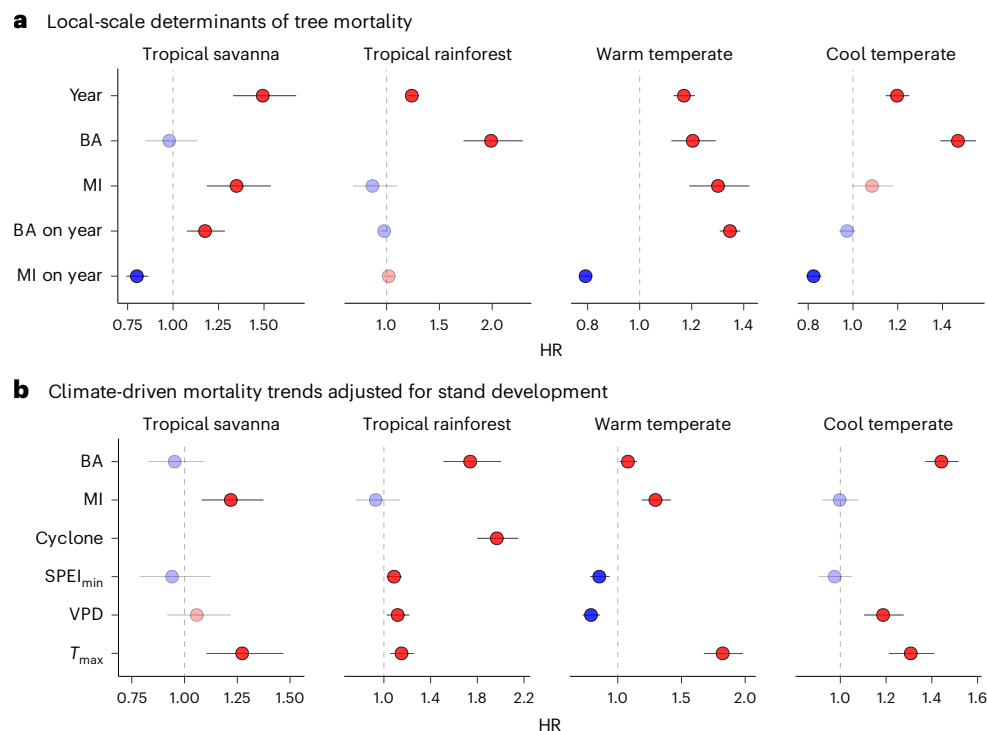


Fig. 2 | Drivers of tree mortality across four major forest biomes in Australia.

a, Fixed effects of stand structure and local mean climate on average mortality rates and their temporal trends. Predictors include year, log-transformed stand basal area (BA) at the start of each census interval and a spatial moisture index (MI). The interactions of BA and MI with year test whether temporal increases in mortality are accelerated in denser stands or drier locations. **b**, Fixed effects of recent climate variability on mortality trends after accounting for structural

and baseline climatic differences among plots. Climatic drivers include tropical cyclone occurrence (cyclone), drought intensity ($SPEI_{min}$), and anomalies of T_{max} and VPD. Lower $SPEI_{min}$ values indicate more severe drought. The hazard ratios (HR; exponentiated coefficients) show multiplicative effects with 95% CIs, where $HR > 1$ (red) denotes elevated and $HR < 1$ (blue) reduced mortality. The sample sizes were 198 tropical savanna plots, 25 tropical rainforest plots, 1,168 warm temperate plots and 1,333 cool temperate plots.

while the other three forest biomes each averaged around 0.01 yr^{-1} (Extended Data Fig. 1). Study duration varied across biomes, ranging from 25 years in tropical savannas to 83 years in warm temperate forests, with a mean duration of 57 ± 23 years. These time trends were based on a changing set of plots over the study period, with a notable drop in plot numbers after the 2000s, especially in temperate biomes (Extended Data Fig. 2). Our results were robust to shifts in the spatial configuration of the plot network (Supplementary Discussion and Supplementary Figs. 1–4), as demonstrated by a plot-by-plot analysis showing increased mortality in over 70% of plots with at least three censuses (Extended Data Fig. 3). The widespread increases in mortality rates indicates that regional-scale demographic changes are underway across the Australian forest biomes.

Plot-level differences in mortality rates and the pace of their temporal change exhibited distinct spatial patterns associated with local mean climate and structural attributes of the forest stands (Fig. 2a). Across biomes, elevated stand basal area was positively associated with higher mortality rates in all forest ecosystems except tropical savannas, where forests are relatively open. In tropical rainforests and cool temperate forests, plot-specific average mortality rates showed no sensitivity to spatial variation in moisture availability. By contrast, the other two biomes had higher mortality in plots with greater long-term moisture availability, probably reflecting the dominance of acquisitive species with rapid growth and shorter lifespans in wetter environments³³. The temporal interaction further showed that, for all biomes except tropical rainforests, mortality increased more sharply over time in historically drier plots. Moreover, in tropical savannas and warm temperate forests, the rise in mortality through time was more pronounced in plots with higher stand basal area.

Competition has been identified as a primary regulator of forest dynamics, but its ability to explain temporal variations in mortality rates across broader landscapes is limited^{34–36}. To assess the role of stand development in our dataset, we tracked plot-level dynamics for a subset of plots with at least three censuses and constant plot areas. In disturbance-mediated temperate systems, we observed increasing stand basal area over time, whereas tree density showed no consistent directional trend (Supplementary Figs. 5–7). This dynamic basal area pattern, with its marked impact on mortality, suggests that self-thinning has left a distinct demographic imprint on mortality patterns in these forests. Nonetheless, self-thinning is not a plausible explanation for the increasing mortality trend we observed. If it were, then controlling for stand basal area should remove the temporal signal in mortality³⁷. However, we found a significant positive mortality trend remained robust even after accounting for basal area, indicating that forest recovery dynamics are insufficient to explain the long-term acceleration in mortality detected at landscape scales (Supplementary Discussion).

When local mean climate and changes in forest structures were statistically controlled for, high temperature emerged as the strongest climatic predictor of tree mortality across biomes (Fig. 2b and Supplementary Table 4). In comparison, severe drought, quantified by low $SPEI_{min}$ values, significantly contributed to higher mortality rates in warm temperate forests only, and positive VPD anomalies increased mortality in tropical rainforests and cool temperate forests only. Acute heat stress can induce direct foliar damage³⁸ and metabolic imbalance by inhibiting photosynthetic enzyme activity while increasing respiratory carbon loss when temperatures exceed thermal optima, even without extreme drought³⁹. Simultaneously, warming-induced increases in atmospheric water demand and soil moisture

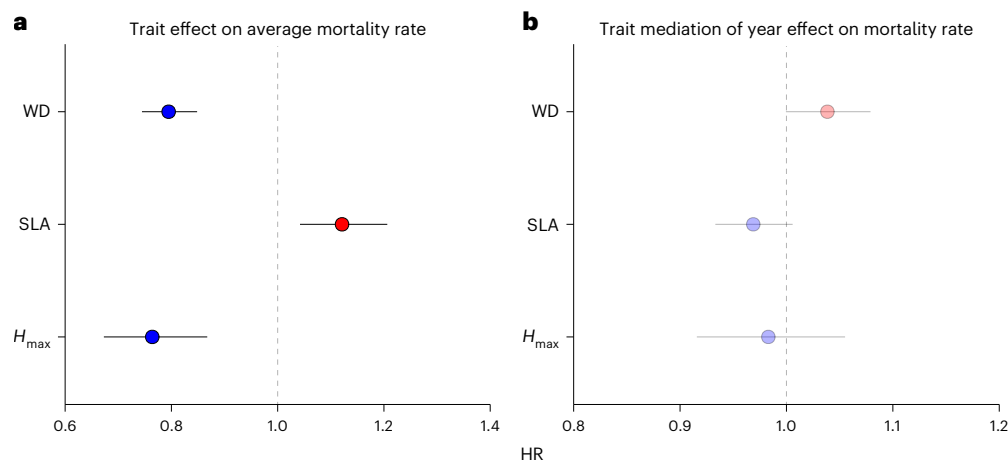


Fig. 3 | Functional traits mediate species-level mortality rates and their temporal trends across four major forest biomes in Australia. a, The fixed effects of maximum tree height (H_{max}), SLA and WD on average species-level mortality rates. **b**, Trait effects on temporal mortality trends. Hazard ratios (HR; points) show multiplicative changes in mortality per 1 s.d. increase in standardized trait values. The error bars denote 95% CIs; the faded points

indicate non-significant effects (CIs overlap HR of 1; dashed line). Each trait was modelled separately. In **a**, an HR >1 (red) indicates higher and HR <1 (blue) lower average mortality rates with increasing trait values. In **b**, an HR >1 indicates stronger and HR <1 weaker temporal increase in mortality rates associated with higher trait values. Sample sizes were 889, 561 and 662 species for H_{max} , SLA and WD, respectively.

depletion can steepen the water potential gradient along the soil–atmosphere continuum, thereby raising the risk of hydraulic failure and desiccation-induced mortality^{9,40–44}. We also noted tight couplings of VPD and SPEI with temperature (Supplementary Fig. 8), which underscores that temperature anomalies exert mortality effects through both direct physiological stresses and indirect hydrological pathways mediated by changes in atmospheric moisture demand and drought intensity. Empirical and experimental evidence from Australian tropical rainforests and temperate forests supports this interpretation, demonstrating that hotter drought conditions probably thermally amplify stress on trees, leading to a reduction in forest carrying capacity across a diversity of stand structures^{36,45}. Long-term climatic records further show a continent-wide trajectory of rising temperature and VPD, coupled with intensified drought (declining SPEI_{min}) in all non-rainforest biomes (Extended Data Figs. 4–6). These trends signal a shift towards a climate regime that compounds warming and drying stresses on Australian forests. Collectively, our findings point to warmer temperatures as the dominant driver of long-term increases in mortality, through a combination of temperature-driven metabolic stress and hydrological impacts. In tropical rainforests, cyclones were an additional significant contributor to tree mortality. Census intervals with cyclones had mortality rates 1.97× higher than unaffected censuses in this biome (95% CI 1.80–2.15) (Fig. 2b and Supplementary Table 4). The pronounced damage caused by cyclones suggests that long-term tropical tree mortality results not from isolated factors but from cascading interactions between episodic disturbances and chronic climate pressures that progressively erode forest resilience and drive functional changes in tropical rainforest ecosystems^{46,47}.

Effects of species functional traits on tree mortality

To examine how functional traits mediate mortality patterns across species over time, we developed three individual-based models for maximum tree height, specific leaf area (SLA) and wood density (WD). This trait-based analysis encompassed more than 87% of individuals from over 560 species, representing over 59% of the species in our mortality datasets (Supplementary Fig. 9). All three traits were significant predictors of interspecific variation in mortality (Fig. 3a). Species with shorter maximum height, higher SLA and lower WD consistently exhibited greater mortality (Extended Data Fig. 7). The mortality response to WD and SLA reflects a trade-off, whereby species that allocate resources

towards rapid growth reduce their investment in structural and hydraulic reinforcement (Extended Data Fig. 8), increasing their vulnerability to mortality under environmental stressors^{48,49}. Maximum tree size, which captures a distinct functional axis, was negatively correlated with tree mortality. This aligns with evidence that taller, long-lived trees generally exhibit lower mortality rates⁵⁰, potentially due to structural advantages such as extensive root systems⁵¹, greater xylem efficiency⁵² and superior light interception for carbon assimilation⁵³. Although over 95% of the species analysed showed rising mortality over time, we found no evidence that specific traits were linked to this temporal trend (Fig. 3b). This indicates that while trait-mediated life-history strategies may reduce baseline mortality rates, they do not confer resistance to the decadal-scale increase in mortality. Moreover, the similar rate of mortality increase over time across species with divergent life-history strategies, ranging from resource-acquisitive to conservative strategies (Extended Data Fig. 9), rules out the possibility that a community-wide shift towards faster-growing and short-lived species underlies the long-term rise in mortality.

Size-dependent tree mortality

At the individual tree level, mortality patterns demonstrated notable size dependency that varied across biomes. In tropical savannas, a U-shaped size-mortality relationship indicated that both small and large trees had higher mortality (Fig. 4a). However, there was no discernible size-related mortality trend for tropical rainforest trees (Fig. 4b). The lack of a size-mortality relationship in tropical rainforests is likely associated with high species-level variation in maximum size, which obscures community-level patterns, as individual species tend to exhibit increasing mortality beyond mid-size stages⁵⁴. In temperate forests, small trees exhibited the highest mortality rates, with trees in warm temperate zones showing an initial decline in mortality with tree size followed by a modest increase (Fig. 4c). In cool zones, mortality decreased exponentially with increasing tree size, eventually leveling off at larger sizes (Fig. 4d). Such high diversity of size-mortality patterns has been identified in forests around the world^{55,56}, highlighting the size-dependent processes that drive tree mortality and ultimately determine their impact on vegetation structure⁵⁷. Small trees generally exhibit high mortality rates due to biotic pressures such as size-asymmetric competition for light and nutrients^{58,59} and high susceptibility to herbivory⁶⁰. Conversely, the mortality of large trees is more closely tied to local environmental conditions and disturbance

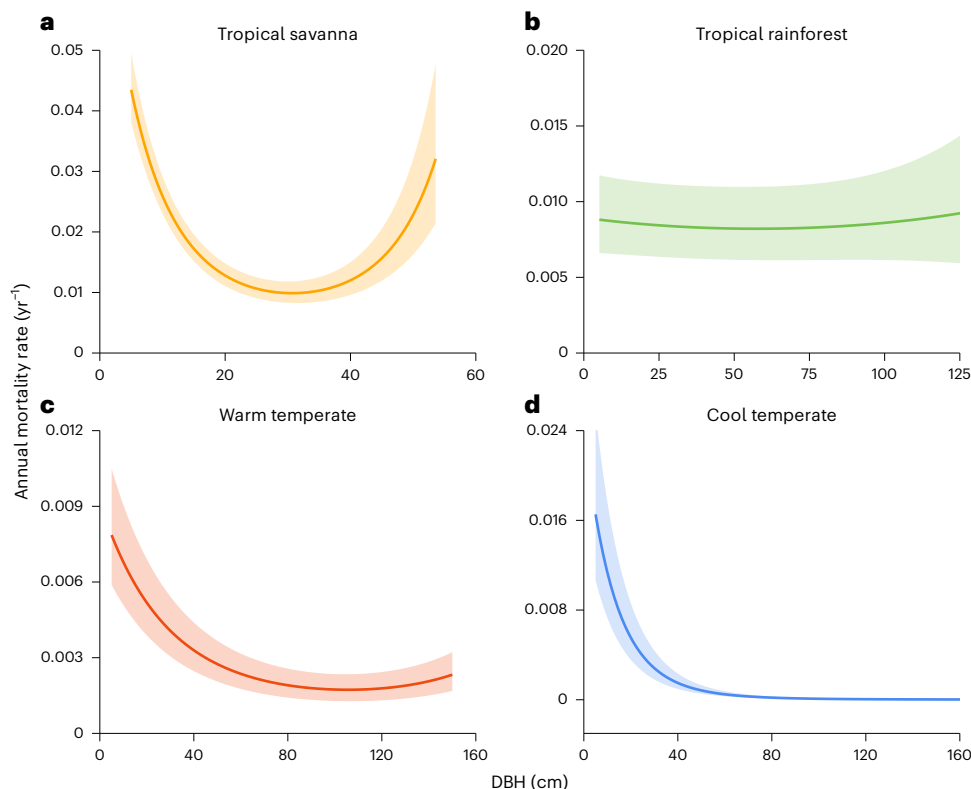


Fig. 4 | Size-dependent tree mortality across four major forest biomes in Australia. a–d. The modelled mean annual mortality rates as a function of tree diameter at breast height are shown for tropical savanna (a), tropical rainforest

(b), warm temperate forest (c) and cool temperate forest (d). The solid lines indicate model predictions, and the shaded areas denote the 95% CIs. The curves extend to the 99.9th percentile of observed DBH to exclude extreme outliers.

regimes specific to each biome^{61,62}. Although larger trees have thicker bark that reduces immediate fire-induced mortality^{60,63}, they often succumb years later to cumulative drought stress⁶⁴ and fire-induced physiological damage⁶⁵. This interaction between fire and drought explains the U-shaped size-dependent response observed in tropical savannas^{66,67}. Cross-biome variation in large-tree mortality may also reflect climate-driven differences in life-history strategy, with evidence showing that lower temperatures promote conservative growth and longer lifespans^{68,69}. Although size-mortality relationships were treated as time-invariant in our models, their pronounced spatial variability across biomes underscores the importance of environmental context in modulating size-dependent mortality drivers. This variation has profound implications for forest carbon dynamics, as mortality of large trees disproportionately affects biomass stocks and carbon residence time⁵⁷.

Trends in forest growth dynamics

To explore whether the long-term increase in mortality could be explained by accelerated growth dynamics, we examined temporal trends in tree-level diameter growth rates and stand-level basal area increment across biomes. Individual growth rates declined with increasing stand basal area across biomes (Extended Data Fig. 10a), consistent with self-thinning dynamics driven by intensified competition for light and soil resources in densely stocked forests^{70–72}. By contrast, the effects of tree size on tree growth were weaker and varied among biomes. Specifically, tree growth rates decreased with tree size in tropical savannas, increased in tropical rainforests and cool temperate forests, and showed no size dependence in warm temperate forests (Extended Data Fig. 10a). After stand basal area and tree size were accounted for, long-term declines in tree growth rates were evident in tropical savannas and cool temperate forests, whereas no discernible trend was detected in tropical rainforests and a modest

increase occurred in warm temperate forests (Extended Data Fig. 10b). At the stand level, higher forest productivity, indicated by stand-level basal area increment, was associated with greater existing stand basal area (Fig. 5a). Temporal analyses that controlled for this relationship further revealed long-term declines in stand-level basal area increment across most biomes, with tropical rainforests showing no significant trend (Fig. 5b). Our analysis of parallel patterns in growth and mortality does not establish a direct causal relationship. However, the lack of a widespread increase in growth suggests that accelerated growth dynamics, through demographic feedbacks due to physiological turnover or competition-induced stresses^{34,35}, are unlikely to explain the observed increases in mortality.

Implications

In summary, our study provides evidence of a continent-wide increase in tree mortality rates over time across four major forest biomes in Australia. These increasing trends persist even after accounting for vegetation dynamics such as competition-driven mortality associated with increasing basal area. We attribute the rising mortality across biomes primarily to warmer temperatures. This climate-mediated increase in mortality, in concert with declining productivity, suggests a progressive weakening of the forest carbon sink. The widespread demographic shifts documented in our study demonstrate that climate change is imposing physiological stress even on historically resilient forests. As climate stressors are projected to intensify towards the late twenty-first century^{73,74}, changes in forest vegetation dynamics are expected to accelerate globally, with potentially severe consequences for forest-climate feedbacks.

Many state-of-the-art dynamic global vegetation models (for example, CLM-FATES, CLM(ED), ED2, LM3-PPA and LPJ-GUESS) simulate forest dynamics using size-structured and cohort-based population demography. However, model representations of tree mortality remain

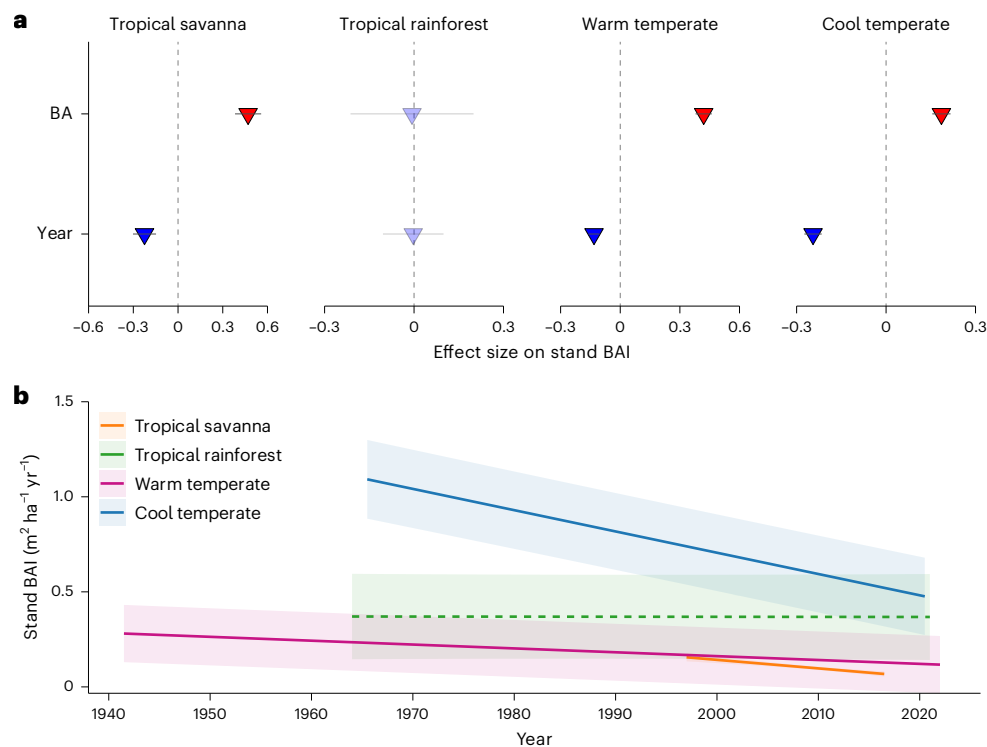


Fig. 5 | Temporal trends in stand basal area increment and their dependence on stand structural attributes across four major forest biomes in Australia.
a. Fixed effects of stand basal area (BA) and year on stand basal area increment.

The red and blue triangles indicate positive and negative effects, respectively. **b.** The modelled mean basal area increment over time (solid line) with the 95% CIs (shaded areas). The dashed lines mark biomes without significant trends.

largely theoretical and poorly constrained by observations, showing large disagreement with observed patterns of mortality and carbon loss^{15,75,76}. The multispecies, cross-biome mortality patterns and drivers identified in our study provide critical benchmarks for evaluating mechanisms assumed to drive tree mortality in models. For instance, the strong empirical relationship between stand basal area and mortality in closed-canopy forests and distinct size-dependent mortality patterns can help refine crowding and resource limitation assumptions in self-thinning formulations. Given the increasingly important role of extreme climate events in driving global tree mortality, our analysis of mortality sensitivities to key climate factors can guide the modelling of climate–mortality interactions. Furthermore, our trait-mortality correlations can enhance representation of diverse tree life-history strategies among plant functional types^{77,78}. These benchmarks establish process-informed targets for assessing whether the emergent behaviour of DGVMs reflects realistic demographic responses to competition and climate extremes. We highlight that long-term forest monitoring plots are indispensable not only for documenting ecosystem change but also for diagnosing and developing dynamic vegetation models to better predict vegetation trajectory and carbon-climate feedback.

Our results also have direct implications for forest management and climate policy in Australia. Government carbon payment initiatives, first the Emissions Reduction Fund and now the Australian Carbon Credit Units scheme, offer financial incentives to landholders and forest managers to conserve and enhance carbon stocks in forests. However, the carbon accounting models underpinning these programmes remain highly uncertain due to incomplete and temporally inconsistent data on tree mortality⁷⁹. Our results indicate that ecosystem models failing to simulate increasing tree mortality rates will overestimate forest carbon sink strength, potentially leading to the misallocation of carbon credits and undermining climate mitigation efforts. Our assessment of historical demographic change here could benchmark existing forest biomass estimates to better capture

transient carbon storage dynamics in terrestrial ecosystems. However, since the early 2000s, the capacity to detect and interpret recent trends in tree mortality across temperate biomes has been increasingly constrained by the decline of long-term forest monitoring programmes (Extended Data Fig. 2). In temperate biomes, the loss of monitoring plots has resulted from a combination of financial, technological and environmental factors. One major driver has been land tenure changes, particularly the reclassification of managed native forests into national parks, which often removed financial incentives and institutional support needed to maintain continuous monitoring. Second, funding cuts associated with institutional restructuring, such as the corporatization of State Forests of New South Wales (NSW) into the Forestry Corporation of NSW, have resulted in fewer active plots and extended measurement intervals. Third, technological innovations in remote sensing have prompted Forestry Tasmania to adopt airborne LiDAR surveys in place of labour-intensive ground surveys for forest management⁸⁰, a valuable innovation, but one that presents challenges for detecting long-term change. Lastly, severe wildfires have caused a cumulative loss of 187 plot-census records since 2000 and 404 in total, compromising the temporal resolution of temperate forest observations. So far, long-term forest inventories remain the most reliable source of data for tracking individual tree mortality and growth dynamics, both in space and time. We thus advocate for the continuous maintenance of permanent plots as critical international research infrastructure and the establishment of a spatially representative monitoring network that spans broad ecological gradients to support reliable cross-biome comparisons and improve ecological forecasts for forest ecosystems⁸¹.

Methods

Forest plot database

We compiled data from 2,724 plots across Australia (Supplementary Table 1), sourced from 12 long-term forest monitoring networks distributed throughout the country, including state forest inventory

programmes in Queensland (QLD), NSW, Victoria, Western Australia and Tasmania; ecological monitoring networks in Victoria; and ecological research plots in the Northern Territory and QLD (for example, QPRP-CSIRO, QPRP-Connell and TERN). These datasets vary in their sampling protocols, temporal coverage and census intervals; full metadata details are provided in Supplementary Tables 2 and 3. Individual plots were censused over varying time intervals, with the combined dataset spanning 1941–2023. Typically, all trees within each plot with diameter at breast height (DBH) ≥ 5 cm or ≥ 10 cm, as specified by the respective plot protocol, were tagged, recorded and remeasured at irregular intervals (mean \pm s.d. of 5 ± 4 years, range of 1–25 years). Plot sizes ranged from 0.04 to 2 ha. Each plot was surveyed between 2 and 29 times. The cumulative plot area sampled across biomes totalled 41.3 ha in tropical savanna, 15.1 ha in tropical rainforest, 533 ha in warm temperate forest and 278 ha in cool temperate forest.

For our analysis, forest plots were selected based on the following criteria: (1) plots were at least 0.04 hectares in size. (2) Trees with a DBH ≥ 5 cm that had been measured at least twice and had not been logged or died from fire were included. (3) Plots experiencing complete mortality (that is, 100% tree loss) were omitted to isolate mortality patterns from abrupt, large-scale abiotic disturbances. (4) At least 1 year had elapsed between inventories to track interannual mortality changes. For plots surveyed multiple times within a single year, subannual surveys were aggregated, and survival status was determined based on the final observation of that year. (5) Only censuses with at least ten trees were included to minimize stochastic noise in per-capita mortality rate calculations. (6) Plots had accurate geographic coordinates for extracting climate variables. For most Australian inventories included in our study, plot locations were recorded using GPS-derived Universal Transverse Mercator coordinates referenced to the Geocentric Datum of Australia 1994 (GDA94). Coordinates consisted of six-digit Easting and seven-digit Northing values, providing a spatial resolution of approximately 1 m and a positional accuracy generally within ± 10 m under field conditions. For a small subset of the VicForests permanent growth plots (86 of 349) without precise geographic coordinates, the centroid of the corresponding forest management zone was used as a proxy. In each plot, any missing intervals between consecutive tree records were inferred based on the tree's status before and after the gap. Specifically, we implemented procedures for assessing tree recovery after disturbances: (1) trees initially recorded as dead but later resprouting and recorded as alive were classified as alive. (2) Trees that switched between dead and alive in consecutive censuses were considered dead based on the latest record. (3) For a tree's last alive status followed by a missing interval and then a dead record, the death was assumed to have occurred during the first missing census.

Climate data

The SPEI (unitless) is a multiscale drought metric that quantifies climatic water balance anomalies by calculating the standardized difference between precipitation and potential evapotranspiration (PET), the latter estimated using the Penman–Monteith approach⁸². We used the 12-month SPEI derived from the Climatic Research Unit dataset (SPEIbase v.2.10), with a spatial resolution of 0.5° , covering the period from 1901 to 2023. To quantify drought stress during census intervals, we calculated SPEI_{min}, defined as the average of the annual minimum monthly SPEI value within each interval. To characterize the spatial variation in background hydroclimate among plots, we used a moisture index (MI, unitless), defined as the 30-year (1970–2000) mean annual precipitation divided by PET. The MI values were retrieved as an aridity index from the CGIAR-CSI Global Aridity and Global PET database v2, at approximately 1 km resolution. The moisture index is often referred to as the aridity index in the literature, but this may cause confusion because higher values correspond to lower aridity. Here, we adopt the term MI following Prentice's work⁸³. Atmospheric

aridity was further evaluated using VPD (in kilopascals), which is calculated based on atmospheric humidity and temperature⁴². Monthly T_{\max} and VPD for each plot were extracted from TerraClimate⁸⁴, a global dataset with approximately 4 km spatial resolution dating back to 1958. All climatic variables were expressed as standardized anomalies relative to the plot-specific long-term mean and standard deviation (1958–2024). For each plot and census interval, we averaged these monthly anomalies for T_{\max} and mean VPD to characterize average thermal and atmospheric water stress corresponding to each census interval. Because Australian tropical ecosystems experience strong monsoonal climates and frequent cyclonic disturbances^{45,47}, we used local historical cyclone records from the Queensland Permanent Rainforest Plot (QPRP) dataset to evaluate their role in shaping mortality patterns. Nevertheless, uncertainties remain in attributing mortality trends to available climate data due to lagged mortality responses and irregular sampling intervals, which may obscure the exact timing of mortality events and complicate causal inference.

Biome classification

Plots were initially classified using the Australian National Vegetation Information System⁸⁵, but preliminary analysis revealed that some plots were labelled as 'unassigned native vegetation' or were mismatched with ground observations. We therefore developed a new classification system based on three key plot-level characteristics: (1) dominant species composition, (2) stand structure and (3) local climate zone. This approach grouped plots into four biomes: tropical savanna, tropical rainforest, warm temperate forest and cool temperate forest. Plots north of 20° S latitude were categorized as tropical, with tropical savannas exhibiting distinct wet and dry seasons and a vegetation structure composed of a woody overstorey and C_4 grasses. By contrast, tropical rainforests in this region were characterized by dense forests of evergreen tree species. One plot from the QPRP-CSIRO dataset located just below 20° S latitude was reclassified from warm temperate forest to tropical rainforest due to its species composition being more consistent with other tropical rainforest plots. Plots between 20° S and 33.5° S were defined as warm temperate forests, and those south of 33.5° S latitude were identified as cool temperate forests.

Excluding fire impacts in mortality analysis

Fire is a fundamental ecological force that shapes Australian terrestrial ecosystems⁸⁶, capable of driving substantial losses of woody biomass across entire plots. To minimize bias in background mortality trends caused by fire events, we excluded any censuses affected by wildfires using the Bushfire Boundaries dataset from the Digital Atlas of Australia. This dataset tracks wildfire events from 1900 to 2023 but does not cover the Northern Territory, parts of which experience frequent wildfires. For the savanna biome, we used a published dataset⁶⁶ containing detailed fire histories for each plot derived from annual aerial photographs collected throughout the monitoring period. Fire events were classified into three severity levels: low, moderate and high. Because prior analyses using this dataset showed sizeable increases in tree mortality following moderate- and high-severity fires⁶⁶, we excluded census periods containing years with such fire events. Although excluding fire-affected censuses does not eliminate the underlying directional mortality trend, this approach introduces greater interannual variability and reduces sample continuity, thereby providing a more conservative estimate of background mortality.

Functional trait data

We selected three key functional traits that are critical for understanding tree survival strategies and are widely available across species⁴⁸. Maximum tree height is a species-level trait associated with light acquisition and diaspore dispersal capacity (H_{\max} , in metres). SLA (in $\text{m}^2 \text{g}^{-1}$) and WD (in mg mm^{-3}) capture contrasting axes of the trade-off

between growth potential and vulnerability to mortality caused by biomechanical or hydraulic failure. Trait values were sourced from the AusTraits database⁸⁷. For SLA and WD, only field-based measurements of adult individuals were included and averaged at the species level. H_{\max} values were based on expert assessments sourced from official floras. Species mean trait values were used to represent the functional characteristics of each species in subsequent analyses.

Mortality rate calculation

The annual mortality rates (in yr^{-1}) were estimated as

$$m = 1 - \left(1 - \frac{N_D}{N_0}\right)^{\frac{1}{\Delta t}}, \quad (1)$$

where m is the annual mortality rate (in yr^{-1}), N_0 indicates the number of trees measured at the start of the interval, N_D is the number of trees that have died during the interval and Δt is the census interval (in years)^{88,89}.

Tree-level diameter growth rate and stand-level basal area increment

Annual growth rates (AGR, in cm yr^{-1}) were calculated for all living trees based on DBH measured at two timepoints t_1 and t_2 , as

$$\text{AGR} = \frac{\text{DBH}_{t_2} - \text{DBH}_{t_1}}{\Delta t}, \quad (2)$$

where DBH_{t_1} and DBH_{t_2} are diameters at breast height (in centimetres) at times t_1 and t_2 , respectively. Δt is the time between measurements (in years). Following the approach of Bauman et al.⁹⁰, negative anomalous tree growth rates were removed when the observed decrease in DBH was greater than four times the estimated measurement error, calculated as

$$\text{DBH}_{t_2} < (\text{DBH}_{t_1}) - 4 \times (0.0062 \times \text{DBH}_{t_2} + 0.904). \quad (3)$$

This DBH-dependent error function (equation (3), in mm), combined with an absolute lower bound of -0.5 cm yr^{-1} , defined the criteria for excluding anomalous decreases⁹¹. These filters resulted in the exclusion of <2% of measurements. For anomalously high growth values, we set an upper threshold at the 95th percentile of the species-specific AGR distribution. Initial analyses revealed a nonlinear response with increasing tree size, saturating around 80 cm DBH^{91,92} (Supplementary Fig. 10). To mitigate this bias and adhere to linear modelling assumptions, our temporal analysis was restricted to trees under 80 cm, which retained 98% of the surviving individuals in the dataset.

Finally, stand-level dynamics were assessed by analysing annual changes in total basal area of all surviving trees, providing complementary insights to individual tree growth patterns. Stand-level basal area increment (in $\text{m}^2 \text{ ha}^{-1} \text{ yr}^{-1}$) was calculated as

$$\text{BAI} = 1/A \sum_{i=1}^n \text{bai}_i, \quad (4)$$

where A is the plot area (in hectares), and bai_i is the basal area increment of tree i (in $\text{m}^2 \text{ yr}^{-1}$), calculated as the difference in basal area between two timepoints divided by the length of the interval

$$\text{bai}_i = \frac{\text{ba}_{t_2} - \text{ba}_{t_1}}{\Delta t}. \quad (5)$$

In this equation, ba_{t_2} and ba_{t_1} are the basal areas of a tree at times t_2 and t_1 , respectively. Only surviving trees (that is, those alive at t_2) are included in the BAI summation. n is the number of such trees in the plot. The sum of individual tree increments is divided by A , the plot area in hectares, to express BAI on a per-hectare basis.

Temporal trend analysis

The identity of plots sampled in our dataset changed through time, with a notable decline in the number of censuses available after the 2000s. This variation has the potential to confound within-plot temporal trends with between-plot differences, and unequal representation of forest types and plot numbers through time could bias aggregated mortality estimates. To account for this plot-switching issue⁹³, we interpolated multiyear mortality rates by distributing them evenly across each year within the corresponding census interval. For years without direct observations, we assumed a constant annual mortality rate equal to the standardized mean rate calculated over that interval. We then performed bootstrapping with 1,000 resamples per year to minimize bias arising from uneven sampling intensity among years. Annual mortality rates were subsequently averaged across plots, weighted by the square root of plot area to account for differences in sample size^{6,94}. Uncertainty in mean temporal trends was quantified as 95% CIs derived from the 2.5th and 97.5th percentiles of the bootstrap distributions.

Statistical models

We used generalized linear mixed-effects models to explore the drivers of average mortality rates and their long-term trends at different scales. We fitted seven sets of models, each applied independently to individual biomes. Model 1 characterized long-term mortality patterns; model 2 tested whether plot-level mean mortality rates and their trends varied along gradients of local climate and stand structure; model 3 evaluated the influence of climate variability on long-term mortality; model 4 analysed species-specific mortality responses to functional traits; model 5 quantified the size dependence of individual tree mortality; model 6 examined temporal trends in tree-level diameter growth and stand-level basal area increment; and model 7 assessed long-term trends in climatic variables (see Supplementary Methods 1 and 2 for details).

Models 1–3 modelled tree mortality using a binomial distribution with a complementary log–log link function to linearize equation (1)⁹⁵. The response variable was structured as a two-column matrix representing the number of tree deaths and survivors per plot per census interval. An offset term, defined as the natural logarithm of the census interval length (years), was included to standardize mortality rates to an annual scale across varying census durations. To account for temporal variations in plot identity and differences in survey protocols across datasets, the model included a random intercept for plots nested within inventory sources. Many forest plots in our network, particularly in temperate biomes, remain in non-equilibrium following historical disturbances such as logging and wildfire, resulting in ongoing stand aggradation and structural change. We therefore modelled temporal mortality trends across plots on different successional trajectories by including mid-census year as a temporal predictor and the log-transformed initial basal area of each interval as a fixed covariate, to account for the confounding effects of forest recovery from past disturbances. This allowed us to test whether tree mortality exhibited a temporal trend beyond natural forest recovery.

To examine the role of local mean climate and dynamic stand structure in mediating both average mortality rates and their temporal changes across plots, model 2 included fixed effects for year, log-transformed stand basal area and a moisture index representing spatial heterogeneity in baseline water availability. Interaction terms with year were included to analyse spatial variation in the rate of long-term mortality trends along gradients of site moisture and stand structure. Given substantial spatiotemporal changes in forest structure, the interaction between stand basal area and year in model 2 was intended to test whether the strength of temporal mortality trends depended on vegetation structure among plots. Specifically, we tested whether forests with higher basal area, typically indicative of structurally denser and more competitive stands, were more susceptible to long-term increases in mortality. Model 3 examined

the effects of tropical cyclones, SPEI_{min}, VPD and temperature, while controlling for effects of stand structure dynamics and spatial climate gradients identified in model 2. All predictors were standardized before model fitting. Multicollinearity was evaluated using variance inflation factors, all of which were <5 for each biome-specific model. To evaluate the importance of each predictor, we performed likelihood ratio tests comparing model fit (Akaike information criterion (AIC)) with and without individual predictors.

In models 4 and 5, species and individual mortality dynamics were modelled using binary individual survival outcomes (0 = alive, 1 = dead) for each census interval, following a Bernoulli distribution. Model 4 focused on the role of species traits in mediating tree mortality, including fixed effects for year, species mean trait and their interaction. The model incorporated random intercepts for plot identity nested within inventory source, random intercepts for species and random slopes for year by species, capturing interspecific differences in baseline mortality and their temporal trajectories. Each trait (H_{max} , SLA and WD) was analysed in a separate model based on the availability of species-level data for each trait. Model 5 assessed size-dependent mortality by including fixed effects for tree diameter (DBH) and its quadratic term (DBH²). Year was included as an additive fixed effect to account for temporal variation. No interaction between DBH and year was included to preserve interpretability of the primary size-mortality relationship. Random intercepts were included for plot identity nested within inventory source. For the cool temperate biome specifically, the model also included a random intercept for tree identity to account for substantial size heterogeneity (Supplementary Fig. 11), which improved model stability and convergence.

Models 6 and 7 quantified temporal changes in individual tree growth rates, stand basal area increment (BAI) and climate variables using Gaussian distributions with identity link functions. Tree growth rates were modelled as a function of year to capture time trends, with natural logarithm of DBH and stand basal area included as additive fixed effects to account for the influence of intrinsic size and stand structure on growth⁹⁶. Random intercepts and slopes for the log-transformed DBH and year were included at the species level to capture species-specific responses to tree size and time. Random intercepts for tree identity were included to account for repeated DBH measurements from the same individuals. Our model structure followed the hierarchical framework proposed by Bauman et al.⁹⁰, which is designed to account for species-specific differences in allometric size-growth relationships and temporal growth responses⁹⁶. Temporal trends in annual BAI were modelled as a function of year and stand basal area, with random intercepts for plot nested within data source. Stand basal area was log-transformed to capture the nonlinear relationship between BA and BAI at a stand scale⁹⁷. Temporal trends in climate variables were modelled with year as a fixed effect, plot identity as a random intercept and a first-order autoregressive correlation structure to account for temporal autocorrelation.

Reporting summary

Further information on research design is available in the Nature Portfolio Reporting Summary linked to this article.

Data availability

The tree-by-tree observations are publicly available via Figshare at <https://doi.org/10.6084/m9.figshare.28407893> (ref. 98). However, some datasets have been anonymized (for example, geographic locations removed) or excluded, as required by dataset custodians (Supplementary Table 1). The records of tropical cyclone events occurring in QPRP-CSIRO plots can be accessed via <https://data.csiro.au/collection/csiro:6638v3>. The Bushfire Boundaries dataset is available from the Digital Atlas of Australia ([Historical Bushfire Boundaries|Historical Bushfire Boundaries|Digital Atlas of Australia](https://data.csiro.au/collection/csiro:6638v3)). For climate, the SPEI dataset is available at https://spei.csic.es/spei_database_2_10.

The moisture index dataset is available at [CGIAR CSI Global Aridity and PET Database](https://data.csiro.au/collection/csiro:6638v3). TerraClimate dataset is available at <https://doi.org/10.1038/sdata.2017.191>. The AusTraits database is available at <https://austraits.org/>.

Code availability

The codes used for this study are available via Figshare at <https://doi.org/10.6084/m9.figshare.28407893> (ref. 98).

References

- Adams, H. D. et al. Climate-induced tree mortality: Earth system consequences. *Eos Trans. Am. Geophys. Union* **91**, 153–154 (2010).
- McDowell, N. G. et al. Pervasive shifts in forest dynamics in a changing world. *Science* **368**, eaaz9463 (2020).
- Ruiz-Benito, P. et al. Climate- and successional-related changes in functional composition of European forests are strongly driven by tree mortality. *Glob. Change Biol.* **23**, 4162–4176 (2017).
- Needham, J. F., Chambers, J., Fisher, R., Knox, R. & Koven, C. D. Forest responses to simulated elevated CO₂ under alternate hypotheses of size- and age-dependent mortality. *Glob. Change Biol.* **26**, 5734–5753 (2020).
- Hiltner, U., Huth, A. & Fischer, R. Importance of the forest state in estimating biomass losses from tropical forests: combining dynamic forest models and remote sensing. *Biogeosciences* **19**, 1891–1911 (2022).
- Brienen, R. J. W. et al. Long-term decline of the Amazon carbon sink. *Nature* **519**, 344–348 (2015).
- Bauman, D. et al. Tropical tree mortality has increased with rising atmospheric water stress. *Nature* **608**, 528–533 (2022).
- van Mantgem, P. J. et al. Widespread increase of tree mortality rates in the western United States. *Science* **323**, 521–524 (2009).
- McDowell, N. G. et al. Multi-scale predictions of massive conifer mortality due to chronic temperature rise. *Nat. Clim. Change* **6**, 295–300 (2015).
- Senf, C. et al. Canopy mortality has doubled in Europe's temperate forests over the last three decades. *Nat. Commun.* **9**, 4978 (2018).
- Peng, C. H. et al. A drought-induced pervasive increase in tree mortality across Canada's boreal forests. *Nat. Clim. Change* **1**, 467–471 (2011).
- Hubau, W. et al. Asynchronous carbon sink saturation in African and Amazonian tropical forests. *Nature* **579**, 80–87 (2020).
- Hammond, W. M. et al. Global field observations of tree die-off reveal hotter-drought fingerprint for Earth's forests. *Nat. Commun.* **13**, 1761 (2022).
- Hartmann, H. et al. Climate change risks to global forest health: emergence of unexpected events of elevated tree mortality worldwide. *Annu. Rev. Plant Biol.* **73**, 673–702 (2022).
- Yu, K. L. et al. Pervasive decreases in living vegetation carbon turnover time across forest climate zones. *Proc. Natl Acad. Sci. USA* **116**, 24662–24667 (2019).
- Ma, Z. H. et al. Regional drought-induced reduction in the biomass carbon sink of Canada's boreal forests. *Proc. Natl Acad. Sci. USA* **109**, 2423–2427 (2012).
- Rammig, A. & Lapola, D. M. The declining tropical carbon sink. *Nat. Clim. Change* **11**, 727–728 (2021).
- Network, I. T. M. Towards a global understanding of tree mortality. *N. Phytol.* **245**, 2377–2392 (2025).
- Pugh, T. A. M. et al. Understanding the uncertainty in global forest carbon turnover. *Biogeosciences* **17**, 3961–3989 (2020).
- Wei, N. et al. Evolution of uncertainty in terrestrial carbon storage in Earth system models from CMIP5 to CMIP6. *J. Clim.* **35**, 5483–5499 (2022).
- Gallagher, R. V., Allen, S. & Wright, I. J. Safety margins and adaptive capacity of vegetation to climate change. *Sci. Rep.* **9**, 8241 (2019).

22. King, A. D., Pitman, A. J., Henley, B. J., Ukkola, A. M. & Brown, J. R. The role of climate variability in Australian drought. *Nat. Clim. Change* **10**, 177–179 (2020).
23. Peters, J. M. R. et al. Living on the edge: A continental-scale assessment of forest vulnerability to drought. *Glob. Change Biol.* **27**, 3620–3641 (2021).
24. Larter, M. et al. Extreme aridity pushes trees to their physical limits. *Plant Physiol.* **168**, 804–807 (2015).
25. Crombie, D., Tippet, J. & Hill, T. Dawn water potential and root depth of trees and understorey species in southwestern Australia. *Aust. J. Bot.* **36**, 621–631 (1988).
26. Myers, B. A. et al. Seasonal variation in water relations of trees of differing leaf phenology in a Wet-dry tropical savanna near Darwin, Northern Australia. *Aust. J. Bot.* **45**, 225–240 (1997).
27. Lawes, M. J. et al. Appraising widespread resprouting but variable levels of postfire seeding in Australian ecosystems: the effect of phylogeny, fire regime and productivity. *Aust. J. Bot.* **70**, 114–130 (2022).
28. Yang, S., Ooi, M. K. J., Falster, D. S. & Cornwell, W. K. Continental-scale empirical evidence for relationships between fire response strategies and fire frequency. *N. Phytol.* **246**, 528–542 (2025).
29. Forzieri, G., Dakos, V., McDowell, N. G., Ramdane, A. & Cescatti, A. Emerging signals of declining forest resilience under climate change. *Nature* **608**, 534–539 (2022).
30. De Kauwe, M. G. et al. Identifying areas at risk of drought-induced tree mortality across South-Eastern Australia. *Glob. Change Biol.* **26**, 5716–5733 (2020).
31. The Dead Tree Detective. *Western Sydney University* (accessed 5 December 2025); <https://biocollect.ala.org.au/acsa/project/index/77285a13-e231-49e8-b212-660c66c74bac>
32. Yan, Y. et al. Climate-induced tree-mortality pulses are obscured by broad-scale and long-term greening. *Nat. Ecol. Evol.* **8**, 912–923 (2024).
33. Esquivel-Muelbert, A. et al. Tree mode of death and mortality risk factors across Amazon forests. *Nat. Commun.* **11**, 5515 (2020).
34. Luo, Y. & Chen, H. Y. H. Observations from old forests underestimate climate change effects on tree mortality. *Nat. Commun.* **4**, 1655 (2013).
35. Luo, Y. & Chen, H. Y. H. Climate change-associated tree mortality increases without decreasing water availability. *Ecol. Lett.* **18**, 1207–1215 (2015).
36. Trouvé, R., Baker, P. J., Ducey, M. J., Robinson, A. P. & Nitschke, C. R. Global warming reduces the carrying capacity of the tallest angiosperm species (*Eucalyptus regnans*). *Nat. Commun.* **16**, 7440 (2025).
37. Thorpe, H. C. & Daniels, L. D. Long-term trends in tree mortality rates in the Alberta foothills are driven by stand development. *Can. J. Res.* **42**, 1687–1696 (2012).
38. Doughty, C. E. et al. Tropical forests are approaching critical temperature thresholds. *Nature* **621**, 105–111 (2023).
39. Ping, J. et al. Enhanced causal effect of ecosystem photosynthesis on respiration during heatwaves. *Sci. Adv.* **9**, eadi6395 (2023).
40. Hicke, J. A. & Zeppel, M. J. B. Climate-driven tree mortality: insights from the pinon pine die-off in the United States. *N. Phytol.* **200**, 301–303 (2013).
41. Grossiord, C. et al. Plant responses to rising vapor pressure deficit. *N. Phytol.* **226**, 1550–1566 (2020).
42. Zhou, S., Zhang, Y., Williams, A. P. & Gentile, P. Projected increases in intensity, frequency, and terrestrial carbon costs of compound drought and aridity events. *Sci. Adv.* **5**, eaau5740 (2019).
43. Will, R. E., Wilson, S. M., Zou, C. B. & Hennessey, T. C. Increased vapor pressure deficit due to higher temperature leads to greater transpiration and faster mortality during drought for tree seedlings common to the forest-grassland ecotone. *N. Phytol.* **200**, 366–374 (2013).
44. McDowell, N. G. & Allen, C. D. Darcy's law predicts widespread forest mortality under climate warming. *Nat. Clim. Change* **5**, 669–672 (2015).
45. Carle, H. et al. Aboveground biomass in Australian tropical forests now a net carbon source. *Nature* **646**, 611–618 (2025).
46. Zuleta, D. et al. Individual tree damage dominates mortality risk factors across six tropical forests. *N. Phytol.* **233**, 705–721 (2021).
47. Murphy, H. T., Bradford, M. G., Dalongeville, A., Ford, A. J. & Metcalfe, D. J. No evidence for long-term increases in biomass and stem density in the tropical rain forests of Australia. *J. Ecol.* **101**, 1589–1597 (2013).
48. Wright, S. J. et al. Functional traits and the growth-mortality trade-off in tropical trees. *Ecology* **91**, 3664–3674 (2010).
49. Ruger, N. et al. Beyond the fast-slow continuum: demographic dimensions structuring a tropical tree community. *Ecol. Lett.* **21**, 1075–1084 (2018).
50. Ruger, N. et al. Demographic trade-offs predict tropical forest dynamics. *Science* **368**, 165–168 (2020).
51. Callahan, R. P. et al. Forest vulnerability to drought controlled by bedrock composition. *Nat. Geosci.* **15**, 714–719 (2022).
52. Liu, H. et al. Hydraulic traits are coordinated with maximum plant height at the global scale. *Sci. Adv.* **5**, eaav1332 (2019).
53. Givnish, T. J., Wong, S. C., Stuart-Williams, H., Holloway-Phillips, M. & Farquhar, G. D. Determinants of maximum tree height in *Eucalyptus* species along a rainfall gradient in Victoria, Australia. *Ecology* **95**, 2991–3007 (2014).
54. Iida, Y. et al. Linking functional traits and demographic rates in a subtropical tree community: the importance of size dependency. *J. Ecol.* **102**, 641–650 (2014).
55. Muller-Landau, H. C. et al. Testing metabolic ecology theory for allometric scaling of tree size, growth and mortality in tropical forests. *Ecol. Lett.* **9**, 575–588 (2006).
56. Piponiot, C. et al. Distribution of biomass dynamics in relation to tree size in forests across the world. *N. Phytol.* **234**, 1664–1677 (2022).
57. Gora, E. M. & Esquivel-Muelbert, A. Implications of size-dependent tree mortality for tropical forest carbon dynamics. *Nat. Plants* **7**, 384–391 (2021).
58. Lu, R. L. et al. The U-shaped pattern of size-dependent mortality and its correlated factors in a subtropical monsoon evergreen forest. *J. Ecol.* **109**, 2421–2433 (2021).
59. Hülsmann, L. et al. Latitudinal patterns in stabilizing density dependence of forest communities. *Nature* **627**, 564–571 (2024).
60. Barrere, J. et al. Functional traits and climate drive interspecific differences in disturbance-induced tree mortality. *Glob. Change Biol.* **29**, 2836–2851 (2023).
61. Coomes, D. A., Duncan, R. P., Allen, R. B. & Truscott, J. Disturbances prevent stem size-density distributions in natural forests from following scaling relationships. *Ecol. Lett.* **6**, 980–989 (2003).
62. Coomes, D. A. & Allen, R. B. Mortality and tree-size distributions in natural mixed-age forests. *J. Ecol.* **95**, 27–40 (2007).
63. Trouvé, R., Osborne, L. & Baker, P. J. The effect of species, size, and fire intensity on tree mortality within a catastrophic bushfire complex. *Ecol. Appl.* **31**, e02383 (2021).
64. Barlow, J., Peres, C. A., Lagan, B. O. & Hugaasen, T. Large tree mortality and the decline of forest biomass following Amazonian wildfires. *Ecol. Lett.* **6**, 6–8 (2003).
65. Bendall, E. R. et al. Demographic change and loss of big trees in resprouting eucalypt forests exposed to megadisturbance. *Glob. Ecol. Biogeogr.* **33**, e13842 (2024).
66. Murphy, B. P. et al. Using a demographic model to project the long-term effects of fire management on tree biomass in Australian savannas. *Ecol. Monogr.* **93**, e1564 (2023).
67. Prior, L. D., Murphy, B. P. & Russell-Smith, J. Environmental and demographic correlates of tree recruitment and mortality in north Australian savannas. *Ecol. Manag.* **257**, 66–74 (2009).

68. Bialic-Murphy, L. et al. The pace of life for forest trees. *Science* **386**, 92–98 (2024).
69. Johnson, D. J. et al. Climate sensitive size-dependent survival in tropical trees. *Nat. Ecol. Evol.* **2**, 1436–1442 (2018).
70. Oliver, C. D. & Larson, B. A. 'Forest Stand Dynamics, Update Edition'. in *Yale School of the Environment Other Publications* 1 (1996); https://elischolar.library.yale.edu/fes_pubs/1
71. Wang, J., Taylor, A. R. & D'Orangeville, L. Warming-induced tree growth may help offset increasing disturbance across the Canadian boreal forest. *Proc. Natl Acad. Sci. USA* **120**, e2212780120 (2023).
72. Trouvé, R., Bontemps, J.-D., Collet, C., Seynave, I. & Lebourgeois, F. Growth partitioning in forest stands is affected by stand density and summer drought in sessile oak and Douglas-fir. *Ecol. Manag.* **334**, 358–368 (2014).
73. Chen, L. et al. Global increase in the occurrence and impact of multiyear droughts. *Science* **387**, 278–284 (2025).
74. Yuan, X. et al. A global transition to flash droughts under climate change. *Science* **380**, 187–191 (2023).
75. Yu, K. L. et al. Field-based tree mortality constraint reduces estimates of model-projected forest carbon sinks. *Nat. Commun.* **13**, 2094 (2022).
76. Bugmann, H. et al. Tree mortality submodels drive simulated long-term forest dynamics: assessing 15 models from the stand to global scale. *Ecosphere* **10**, e02616 (2019).
77. Moorcroft, P. R., Hurtt, G. C. & Pacala, S. W. A method for scaling vegetation dynamics: the ecosystem demography model (ED). *Ecol. Monogr.* **71**, 557–585 (2001).
78. Scheiter, S., Langan, L. & Higgins, S. I. Next-generation dynamic global vegetation models: learning from community ecology. *N. Phytol.* **198**, 957–969 (2013).
79. Forrester, D. I., England, J. R., Paul, K. I. & Roxburgh, S. H. Sensitivity analysis of the FullCAM model: Context dependency and implications for model development to predict Australia's forest carbon stocks. *Ecol. Model.* **489**, 110631 (2024).
80. Case studies forestry and urban tree management projects. *dimap* (accessed 5 December 2025); <https://dimap.asia/forestry-tasmania-usage-of-full-waveform-lidar-in-forestry-taxation/>
81. Anderson-Teixeira, K. J. et al. CTFs-ForestGEO: a worldwide network monitoring forests in an era of global change. *Glob. Change Biol.* **21**, 528–549 (2015).
82. Allen, R. G., Pereira, L. S., Raes, D. & Smith, M. *FAO Irrigation and Drainage Paper No. 56*. Vol. 56, article e156 (Rome: Food and Agriculture Organization of the United Nations, 1998).
83. Prentice, I. C., Villegas-Diaz, R. & Harrison, S. P. Accounting for atmospheric carbon dioxide variations in pollen-based reconstruction of past hydroclimates. *Glob. Planet. Change* **211**, 103790 (2022).
84. Abatzoglou, J. T., Dobrowski, S. Z., Parks, S. A. & Hegewisch, K. C. Data Descriptor: TerraClimate, a high-resolution global dataset of monthly climate and climatic water balance from 1958–2015. *Sci. Data* **5**, 170191 (2018).
85. Australian Government. *National Vegetation Information System Data Products* (Department of Climate Change, Energy, the Environment and Water, accessed 5 December 2025); <https://www.dcceew.gov.au/environment/environment-information-australia/national-vegetation-information-system/data-products>
86. Lynch, A. H. et al. Using the paleorecord to evaluate climate and fire interactions in Australia. *Annu. Rev. Plant Biol.* **35**, 215–239 (2007).
87. Falster, D. et al. AusTraits, a curated plant trait database for the Australian flora. *Sci. Data* **8**, 254 (2021).
88. Sheil, D. & May, R. M. Mortality and recruitment rate evaluations in heterogeneous tropical forests. *J. Ecol.* **84**, 91–100 (1996).
89. Sheil, D., Burslem, D. F. R. P. & Alder, D. The interpretation and misinterpretation of mortality rate measures. *J. Ecol.* **83**, 331–333 (1995).
90. Bauman, D. et al. Tropical tree growth sensitivity to climate is driven by species intrinsic growth rate and leaf traits. *Glob. Change Biol.* **28**, 1414–1432 (2022).
91. Prior, L. D. & Bowman, D. M. J. S. Big eucalypts grow more slowly in a warm climate: evidence of an interaction between tree size and temperature. *Glob. Change Biol.* **20**, 2793–2799 (2014).
92. Prior, L. D. & Bowman, D. M. Across a macro-ecological gradient forest competition is strongest at the most productive sites. *Front. Plant Sci.* **5**, 260 (2014).
93. Phillips, O. L. et al. Pattern and process in Amazon tree turnover, 1976–2001. *Philos. Trans. R. Soc. B* **359**, 381–407 (2004).
94. Muller-Landau, H. C., Detto, M., Chisholm, R. A., Hubbell, S. P. & Condit, R. Detecting and projecting changes in forest biomass from plot data. *For. Glob. Change* **17**, 381–416 (2014).
95. Trouvé, R. & Robinson, A. P. Estimating consignment-level infestation rates from the proportion of consignment that failed border inspection: possibilities and limitations in the presence of overdispersed data. *Risk Anal.* **41**, 992–1003 (2021).
96. Bowman, D. M. J. S., Brienen, R. J. W., Gloor, E., Phillips, O. L. & Prior, L. D. Detecting trends in tree growth: not so simple. *Trends Plant Sci.* **18**, 11–17 (2013).
97. Trouvé, R., Bontemps, J.-D., Collet, C., Seynave, I. & Lebourgeois, F. When do dendrometric rules fail? Insights from 20 years of experimental thinnings on sessile oak in the GIS Coop network. *Ecol. Manag.* **433**, 276–286 (2019).
98. Lu, R. et al. Pervasive increase in tree mortality across the Australian continent. *Figshare* <https://doi.org/10.6084/m9.figshare.28407893> (2025).

Acknowledgements

We thank all collaborators, including those not listed as coauthors, for supporting this work and for their contributions to data collection and management. We thank the Terrestrial Ecosystem Research Network (Daintree Rainforest, Cow Bay and Robson Creek Supersites) and individual scientists, including Lucas Cernusak and Susan Laurance (James Cook University, QLD), for making their measurements openly accessible. The legacy and contribution of past Queensland Government Forestry Departments and staff in data collection, collation and maintenance of QLD Native Forest Permanent Plot data since 1941 is gratefully acknowledged. We thank H. Murphy (CSIRO) for assistance with the QPRP-CSIRO dataset. We acknowledge that the QPRP-CSIRO data is the long-term work of CSIRO staff. We encourage prospective investigators to inform the principal investigators of their intent to use these data in publications. We acknowledge the Department of Energy, Environment and Climate Action, Victoria, for contributing the Victorian Forest Monitoring Program data. We acknowledge the former VicForests for contributing the Victorian Permanent Growth Plot dataset. For Western Australian data, we thank the Forest Management Branch, Department of Biodiversity, Conservation and Attractions and predecessors, especially the work of L. McCaw, M. Rayner and R. Bredahl. R.L. and J.X. were supported by National Key R&D Program of China (grant no. 2022YFF0802104), National Natural Science Foundation of China (grant no. 32325033) and Shanghai Pilot Program for Basic Research (grant no. TQ20220102). The Forest Industries Climate Change Research Fund grant from the Department of Agriculture, Fisheries and Forestry (project no. B0018298 DAFF) to D. Bowman supported the initial collation of much of the data used in this study. R.T. was funded by an Australian Research Council Discovery Project (grant no. DP220103711). B.E.M. and L.J.W. were supported by an Australian Research Council Laureate Fellowship (grant no. FL190100003) awarded to B.E.M.

Author contributions

B.E.M. initially conceptualized the study. B.P.M., H.C., P.T.G., M.J.L., C.M., D.M., R.M., M.R.N., V.J.N., K.R. and S.S. contributed data and

assisted in their interpretation. L.J.W. and B.E.M. collated the datasets with assistance from L.P., P.J.B., D.I.F. and R.T. R.L. harmonized the datasets; led the data analysis with assistance from R.T., L.J.W. and B.E.M; and wrote the first draft of the manuscript. All authors contributed to manuscript revisions.

Competing interests

The authors declare no competing interests.

Additional information

Extended data is available for this paper at <https://doi.org/10.1038/s41477-025-02188-2>.

Supplementary information The online version contains supplementary material available at <https://doi.org/10.1038/s41477-025-02188-2>.

Correspondence and requests for materials should be addressed to Ruiling Lu or Belinda E. Medlyn.

Peer review information *Nature Plants* thanks Roel Brienen and the other, anonymous, reviewer(s) for their contribution to the peer review of this work.

Reprints and permissions information is available at www.nature.com/reprints.


Publisher's note Springer Nature remains neutral with regard to jurisdictional claims in published maps and institutional affiliations.

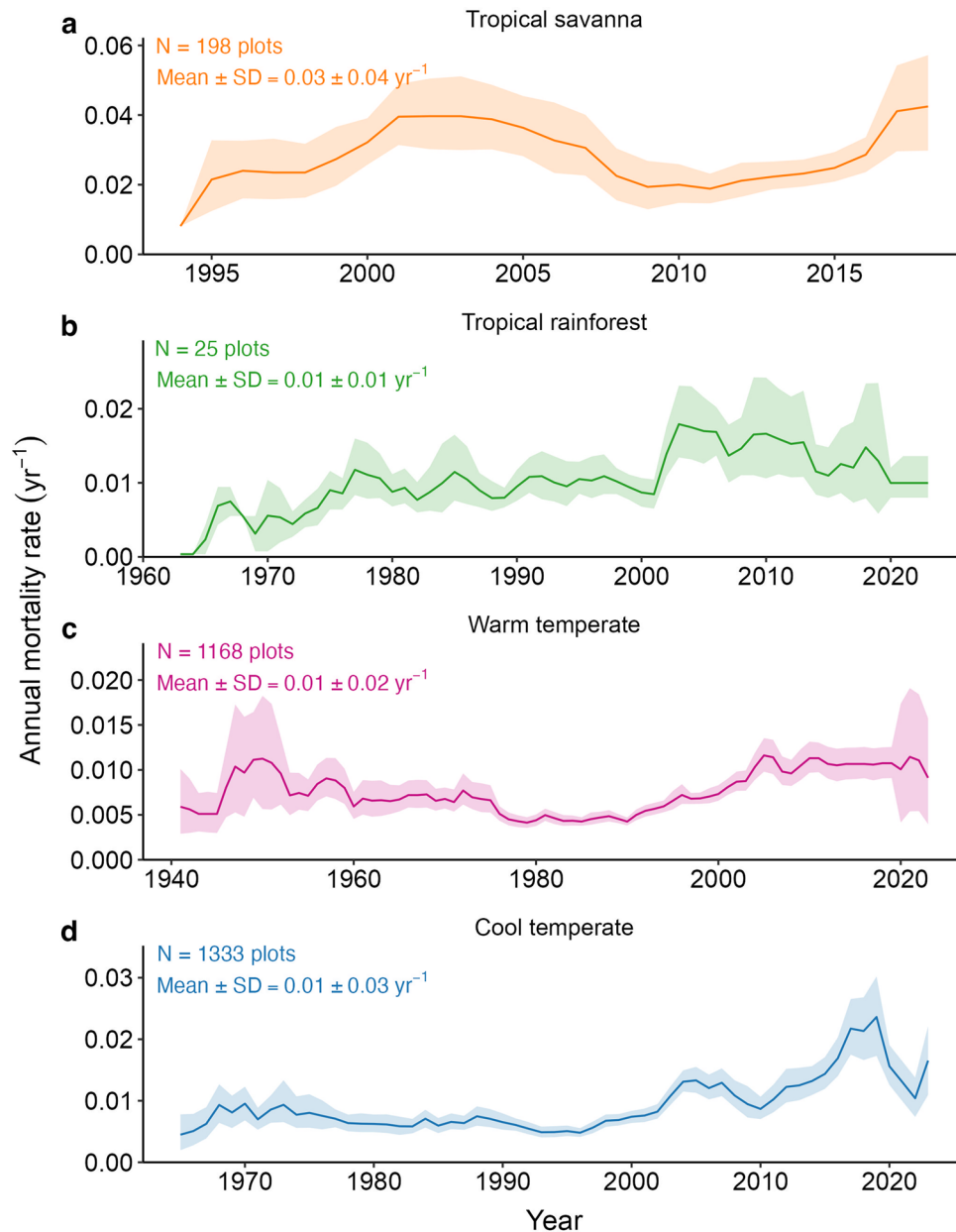
Springer Nature or its licensor (e.g. a society or other partner) holds exclusive rights to this article under a publishing agreement with the author(s) or other rightsholder(s); author self-archiving of the accepted manuscript version of this article is solely governed by the terms of such publishing agreement and applicable law.

© The Author(s), under exclusive licence to Springer Nature Limited 2026

Ruiling Lu ^{1,2} , **Laura J. Williams** ¹, **Raphael Trouvé** ³, **Brett P. Murphy**⁴, **Patrick J. Baker**³, **Hannah Carle** ¹, **David I. Forrester** ⁵, **Peter T. Green**⁶, **Michael J. Liddell**⁷, **Crispen Marunda**⁸, **David Mannes**⁹, **Richard Mazanec**¹⁰, **Michael R. Ngugi** ¹¹, **Victor J. Neldner** ¹¹, **Lynda Prior** ¹², **Katinka X. Ruthrof**^{10,13}, **Shaun Sutor**¹², **Jianyang Xia** ² & **Belinda E. Medlyn** ¹ 

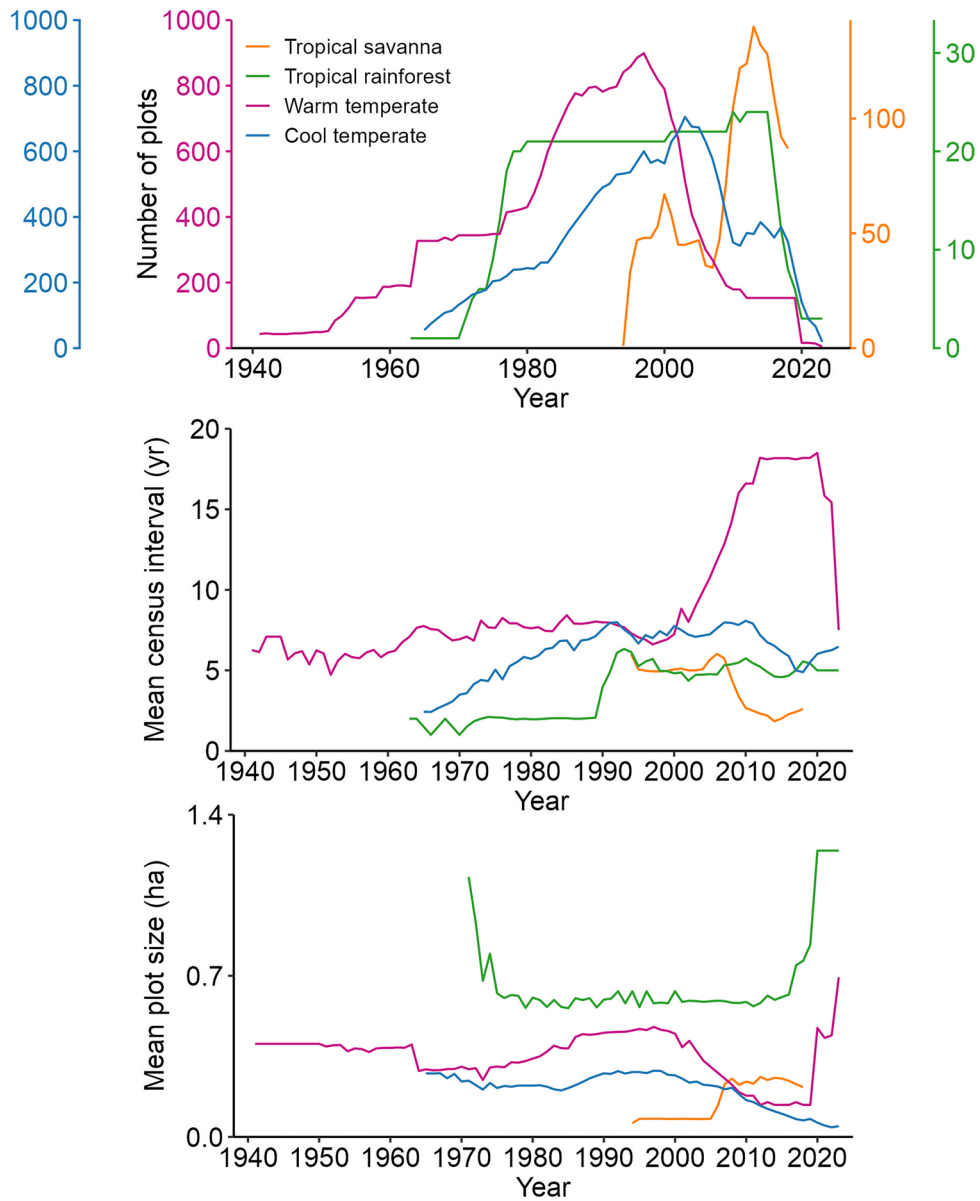
¹Hawkesbury Institute for the Environment, Western Sydney University, Sydney, New South Wales, Australia. ²Research Center for Global Change and Ecological Forecasting, School of Ecological and Environmental Sciences, East China Normal University, Shanghai, China. ³School of Agriculture, Food, and Ecosystem Sciences, The University of Melbourne, Melbourne, Victoria, Australia. ⁴Research Institute for the Environment and Livelihoods, Charles Darwin University, Darwin, Northern Territory, Australia. ⁵CSIRO Environment, Canberra, Australian Capital Territory, Australia. ⁶Department of Environment and Genetics, School of Agriculture, Biomedicine and Environment, La Trobe University, Melbourne, Victoria, Australia. ⁷Centre for Tropical Environmental and Sustainability Science, James Cook University, Cairns, Queensland, Australia. ⁸Sustainable Timber Tasmania, Hobart, Tasmania, Australia. ⁹Forestry Corporation of New South Wales, Sydney, New South Wales, Australia. ¹⁰Biodiversity and Conservation Science, Department of Biodiversity, Conservation and Attractions, Perth, Western Australia, Australia. ¹¹Queensland Herbarium and Biodiversity Science, Department of Environment, Tourism, Science and Innovation, Brisbane, Queensland, Australia. ¹²School of Natural Sciences, University of Tasmania, Hobart, Tasmania, Australia. ¹³School of Environmental and Conservation Sciences, Murdoch University, Murdoch, Western Australia, Australia.

 e-mail: rllu@stu.ecnu.edu.cn; b.medlyn@westernsydney.edu.au

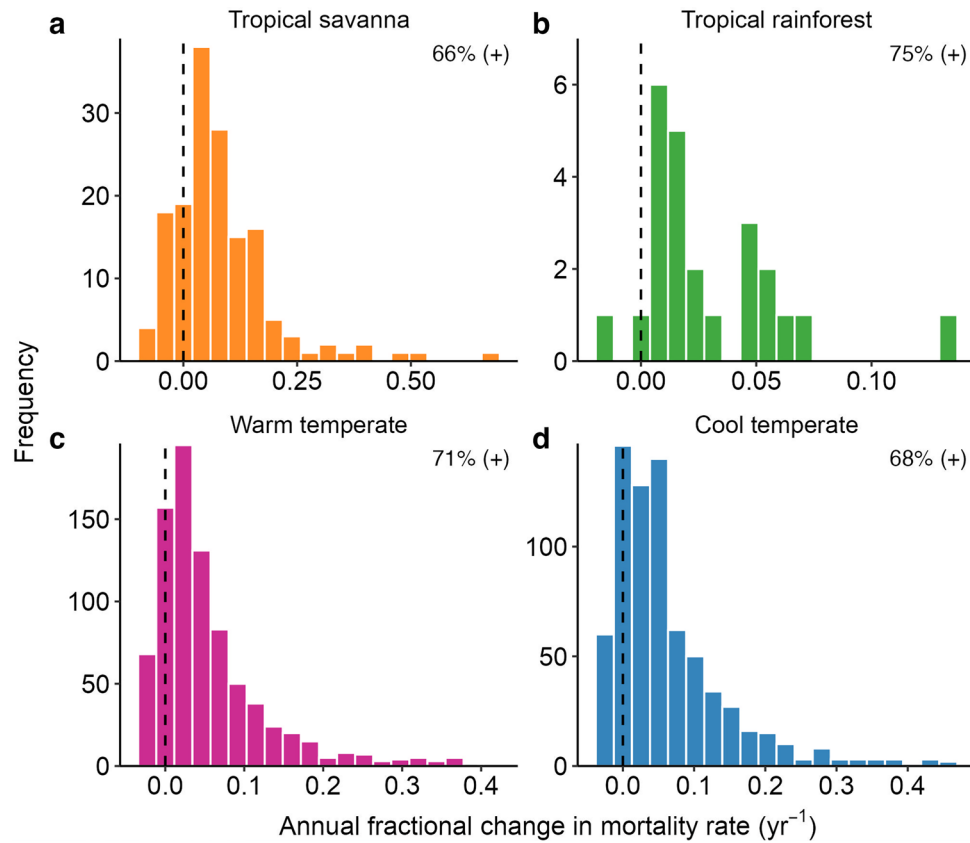


Extended Data Fig. 1 | Temporal pattern of tree mortality rate across four major biomes in Australia. Temporal trajectories of annual tree mortality rate across four major forest biomes: **a**, tropical savanna; **b**, tropical rainforest;

c, warm temperate forest; and **d**, cool temperate forest. Solid lines show mean annual mortality rate, and shaded bands indicate 95% confidence intervals based on 1,000 bootstrap resamples per year.

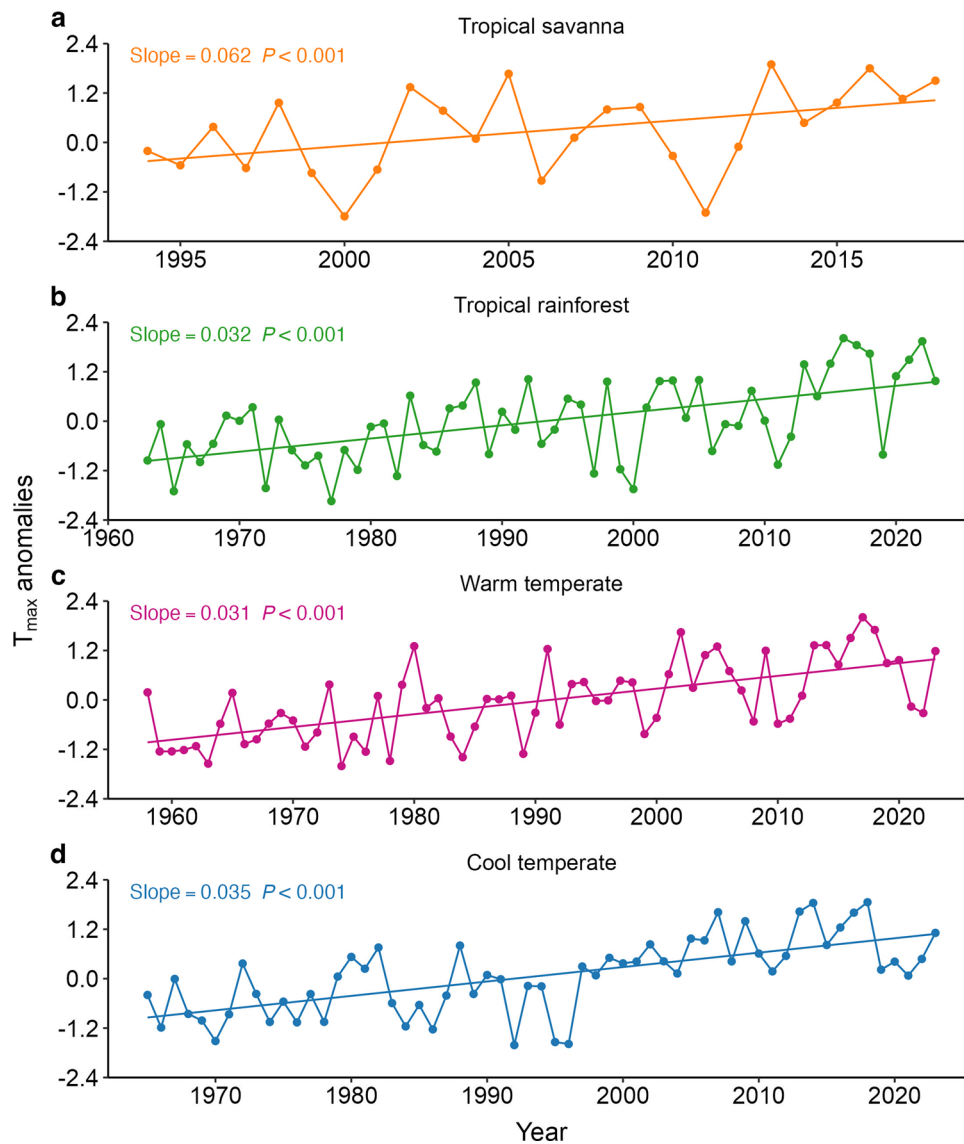


Extended Data Fig. 2 | Temporal variation in plot number, mean plot area, and census interval across four major biomes in Australia. Changes over time in the number of plots, mean plot area, and census interval for four Australian biomes. Colors denote tropical savannas (orange), tropical rainforests (green), warm temperate forests (purple), and cool temperate forests (blue).

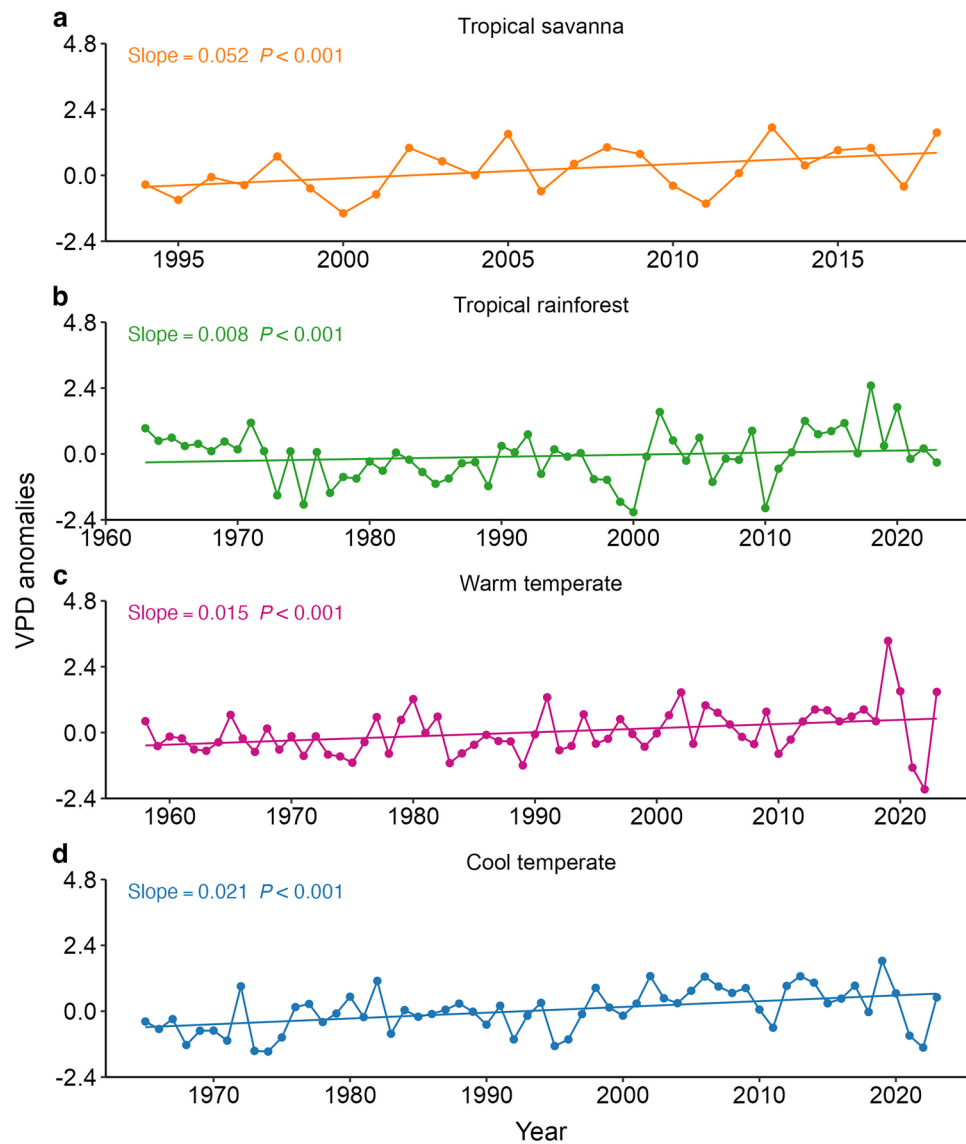


Extended Data Fig. 3 | Plot-level tree mortality trends across four major forest biomes in Australia. Annual change in mortality rate for individual plots in **a**, tropical savanna; **b**, tropical rainforest; **c**, warm temperate forest; and **d**, cool temperate forest. Analyses include only plots with ≥ 3 censuses (sample sizes: 158 of 198, 24 of 25, 895 of 1,168, and 822 of 1,333, respectively). Random-slope

models were fitted to estimate within-plot changes through time, and the annual change in mortality rate was approximated as $\exp(\beta) - 1$, where β is the year coefficient (see Supplementary Methods 1). Plots with β values outside the range -0.5 to 2 were excluded to avoid extreme fits.

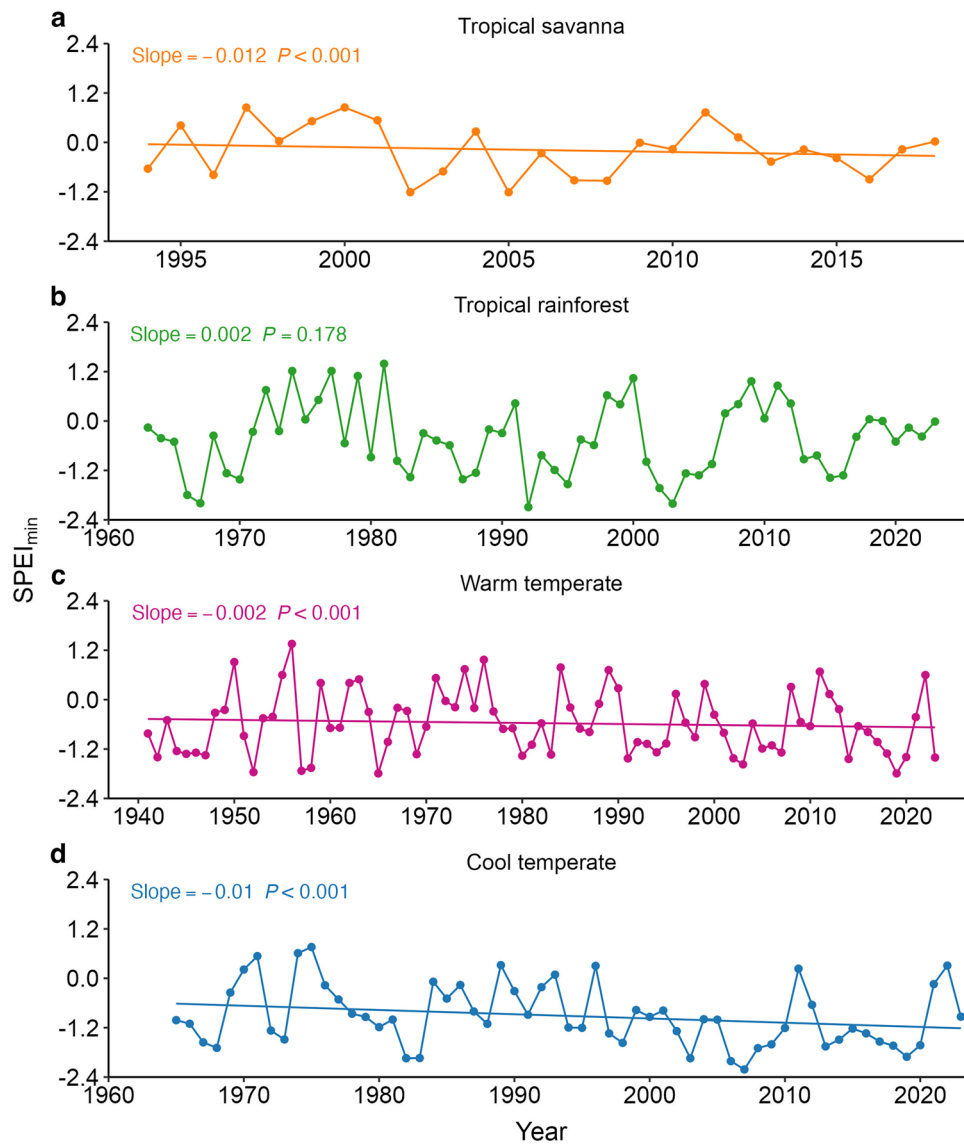


Extended Data Fig. 4 | Temporal trends in annual maximum temperature across four major forest biomes in Australia. Points show the annual mean maximum temperature averaged across plots for **a**, tropical savanna; **b**, tropical rainforest; **c**, warm temperate forest; and **d**, cool temperate forest. Solid lines show the temporal trends predicted by the linear mixed-effects model (Model 7).



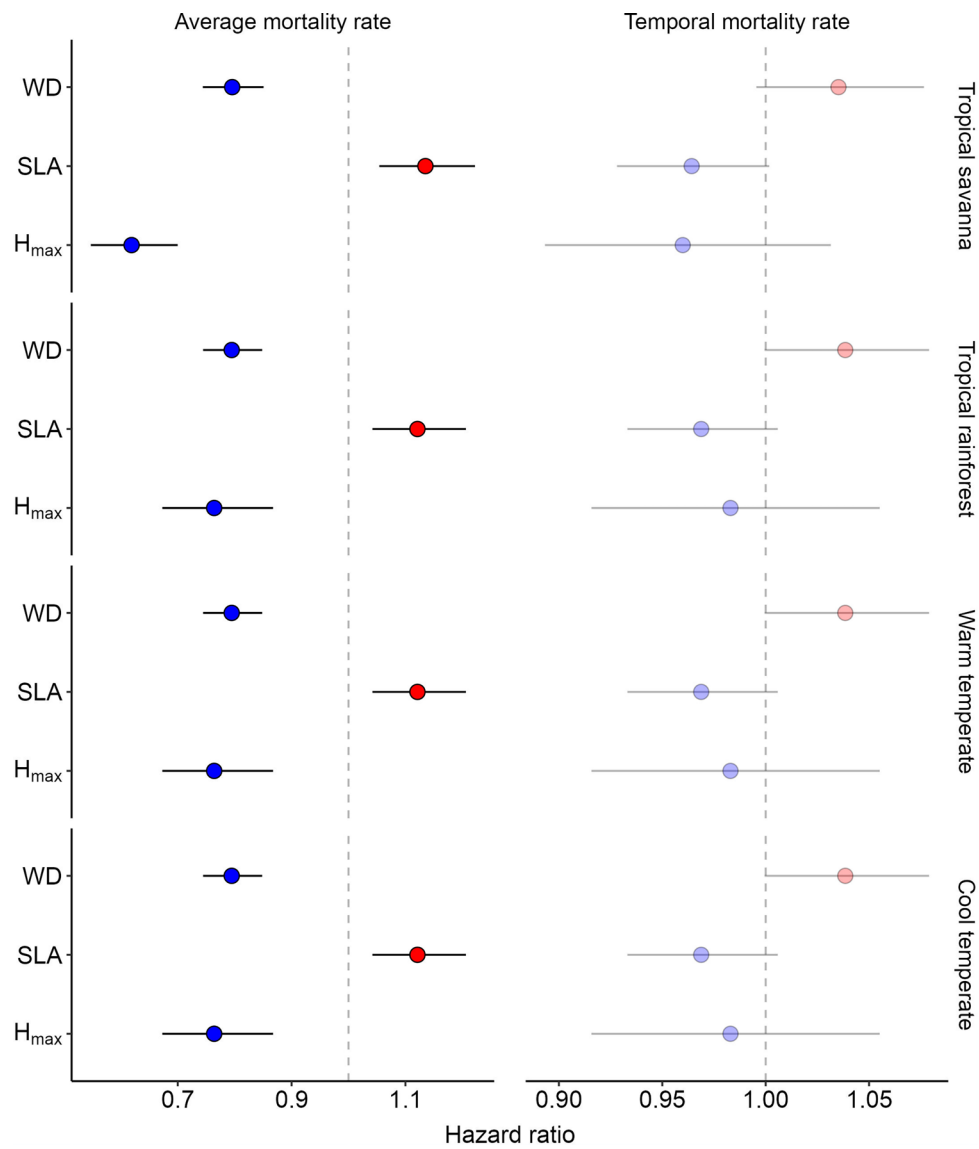
Extended Data Fig. 5 | Temporal trends in annual mean vapor pressure deficit (VPD) across four major forest biomes in Australia. Points show the annual mean vapor pressure deficit (VPD) averaged across plots for **a**, tropical savanna;

b, tropical rainforest; **c**, warm temperate forest; and **d**, cool temperate forest. Solid lines show the temporal trends estimated using a linear mixed-effects model (Model 7).



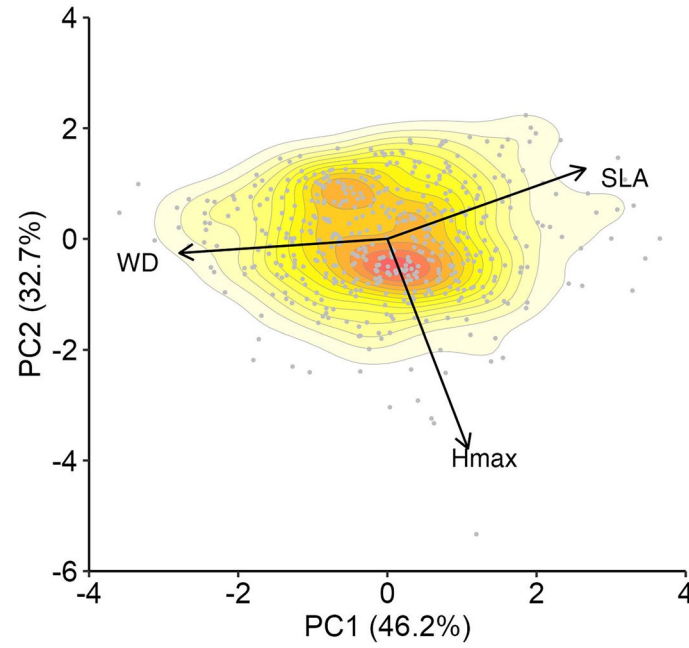
Extended Data Fig. 6 | Temporal trends in drought severity across four major forest biomes in Australia. Points show the annual minimum Standardized Precipitation Evapotranspiration Index (SPEI) averaged across plots for **a**, tropical savanna; **b**, tropical rainforest; **c**, warm temperate forest; and **d**, cool temperate forest. Solid lines show the temporal trends predicted by the linear

mixed-effects model (Model 7). Although SPEI is a relative measure of climatic water balance rather than direct vegetation water loss, sustained negative trends indicate intensifying drought stress and an increasing frequency of extreme drought events.

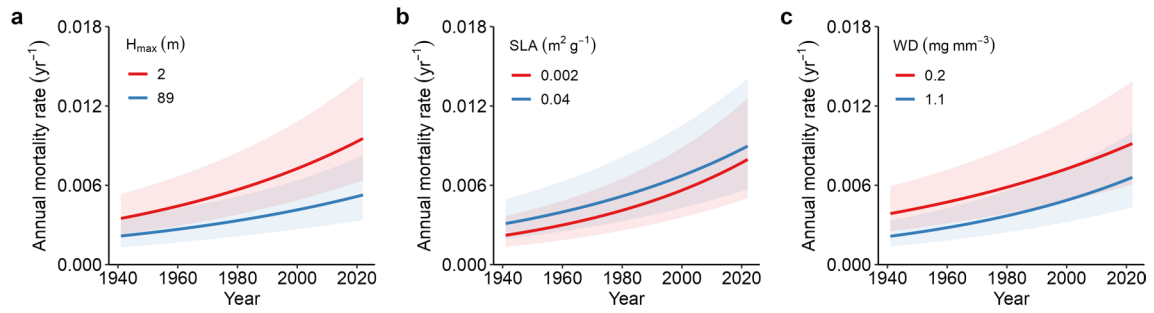


Extended Data Fig. 7 | Trait effects on average mortality rate and temporal change across four major forest biomes in Australia. Effects of species functional traits on average mortality rate and their temporal changes across biomes. Points show estimated hazard ratios with 95% confidence intervals for

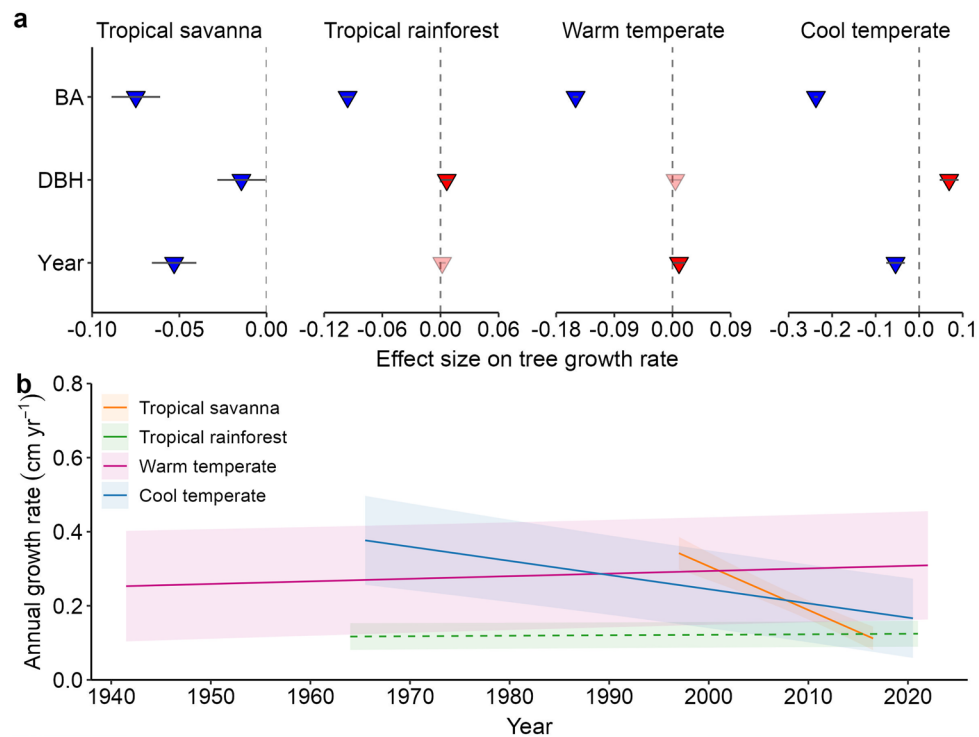
maximum tree height (Hmax), specific leaf area (SLA) and wood density (WD). Traits with positive effects on mortality are shown in red, and those with negative effects in blue. Species numbers were 135 in tropical savannas, 522 in tropical rainforests, 282 in warm temperate forests, and 126 in cool temperate forests.



Extended Data Fig. 8 | Principal component analysis (PCA) of species trait distribution. PCA of species-level mean functional traits. Arrows denote trait loadings, and points represent species mean positions in trait space. Contour lines indicate kernel density of species occurrence, with red showing higher density and yellow lower density.



Extended Data Fig. 9 | Predicted mortality patterns across key functional trait gradients. Modelled temporal mortality patterns across gradients of **a**, maximum tree height (H_{max}); **b**, specific leaf area (SLA); and **c**, wood density (WD) for all biomes combined. Shaded bands indicate 95% confidence intervals for fixed effects.



Extended Data Fig. 10 | Temporal trends in tree growth rate and determinants across four major forest biomes in Australia. Temporal patterns of tree growth rate across four major biomes and their dependence on tree- and stand-level characteristics. **a**, Fixed effects of stand basal area (BA), diameter at breast height (lnDBH), and year on annual tree growth rate. Red and blue triangles denote

significant positive and negative effects, respectively. **b**, Modelled annual tree growth rates over time. Solid lines show significant temporal trends with shaded 95% confidence intervals; dashed lines denote non-significant trends. Trees with DBH > 80 cm (2% of total) were excluded due to nonlinear growth responses not captured by the linear model (see Supplementary Fig. 10).

Reporting Summary

Nature Portfolio wishes to improve the reproducibility of the work that we publish. This form provides structure for consistency and transparency in reporting. For further information on Nature Portfolio policies, see our [Editorial Policies](#) and the [Editorial Policy Checklist](#).

Statistics

For all statistical analyses, confirm that the following items are present in the figure legend, table legend, main text, or Methods section.

- | n/a | Confirmed |
|--------------------------|--|
| <input type="checkbox"/> | <input checked="" type="checkbox"/> The exact sample size (n) for each experimental group/condition, given as a discrete number and unit of measurement |
| <input type="checkbox"/> | <input checked="" type="checkbox"/> A statement on whether measurements were taken from distinct samples or whether the same sample was measured repeatedly |
| <input type="checkbox"/> | <input checked="" type="checkbox"/> The statistical test(s) used AND whether they are one- or two-sided
<i>Only common tests should be described solely by name; describe more complex techniques in the Methods section.</i> |
| <input type="checkbox"/> | <input checked="" type="checkbox"/> A description of all covariates tested |
| <input type="checkbox"/> | <input checked="" type="checkbox"/> A description of any assumptions or corrections, such as tests of normality and adjustment for multiple comparisons |
| <input type="checkbox"/> | <input checked="" type="checkbox"/> A full description of the statistical parameters including central tendency (e.g. means) or other basic estimates (e.g. regression coefficient) AND variation (e.g. standard deviation) or associated estimates of uncertainty (e.g. confidence intervals) |
| <input type="checkbox"/> | <input checked="" type="checkbox"/> For null hypothesis testing, the test statistic (e.g. F , t , r) with confidence intervals, effect sizes, degrees of freedom and P value noted
<i>Give P values as exact values whenever suitable.</i> |
| <input type="checkbox"/> | <input checked="" type="checkbox"/> For Bayesian analysis, information on the choice of priors and Markov chain Monte Carlo settings |
| <input type="checkbox"/> | <input checked="" type="checkbox"/> For hierarchical and complex designs, identification of the appropriate level for tests and full reporting of outcomes |
| <input type="checkbox"/> | <input checked="" type="checkbox"/> Estimates of effect sizes (e.g. Cohen's d , Pearson's r), indicating how they were calculated |

Our web collection on [statistics for biologists](#) contains articles on many of the points above.

Software and code

Policy information about [availability of computer code](#)

Data collection

Data analysis

For manuscripts utilizing custom algorithms or software that are central to the research but not yet described in published literature, software must be made available to editors and reviewers. We strongly encourage code deposition in a community repository (e.g. GitHub). See the Nature Portfolio [guidelines for submitting code & software](#) for further information.

Data

Policy information about [availability of data](#)

All manuscripts must include a [data availability statement](#). This statement should provide the following information, where applicable:

- Accession codes, unique identifiers, or web links for publicly available datasets
- A description of any restrictions on data availability
- For clinical datasets or third party data, please ensure that the statement adheres to our [policy](#)

Research involving human participants, their data, or biological material

Policy information about studies with [human participants or human data](#). See also policy information about [sex, gender \(identity/presentation\), and sexual orientation](#) and [race, ethnicity and racism](#).

Reporting on sex and gender

Use the terms *sex* (biological attribute) and *gender* (shaped by social and cultural circumstances) carefully in order to avoid confusing both terms. Indicate if findings apply to only one sex or gender; describe whether sex and gender were considered in study design; whether sex and/or gender was determined based on self-reporting or assigned and methods used. Provide in the source data disaggregated sex and gender data, where this information has been collected, and if consent has been obtained for sharing of individual-level data; provide overall numbers in this Reporting Summary. Please state if this information has not been collected. Report sex- and gender-based analyses where performed, justify reasons for lack of sex- and gender-based analysis.

Reporting on race, ethnicity, or other socially relevant groupings

Please specify the socially constructed or socially relevant categorization variable(s) used in your manuscript and explain why they were used. Please note that such variables should not be used as proxies for other socially constructed/relevant variables (for example, race or ethnicity should not be used as a proxy for socioeconomic status). Provide clear definitions of the relevant terms used, how they were provided (by the participants/respondents, the researchers, or third parties), and the method(s) used to classify people into the different categories (e.g. self-report, census or administrative data, social media data, etc.) Please provide details about how you controlled for confounding variables in your analyses.

Population characteristics

Describe the covariate-relevant population characteristics of the human research participants (e.g. age, genotypic information, past and current diagnosis and treatment categories). If you filled out the behavioural & social sciences study design questions and have nothing to add here, write "See above."

Recruitment

Describe how participants were recruited. Outline any potential self-selection bias or other biases that may be present and how these are likely to impact results.

Ethics oversight

Identify the organization(s) that approved the study protocol.

Note that full information on the approval of the study protocol must also be provided in the manuscript.

Field-specific reporting

Please select the one below that is the best fit for your research. If you are not sure, read the appropriate sections before making your selection.

Life sciences Behavioural & social sciences Ecological, evolutionary & environmental sciences

For a reference copy of the document with all sections, see [nature.com/documents/nr-reporting-summary-flat.pdf](https://www.nature.com/documents/nr-reporting-summary-flat.pdf)

Ecological, evolutionary & environmental sciences study design

All studies must disclose on these points even when the disclosure is negative.

Study description

Here, we synthesized 83 years of forest inventory data from 2,724 plots across Australian forests to assess long-term tree mortality trends. We show that tree mortality has increased across all major forest biomes over the past eight decades. On average, tree mortality tended to be higher in plots with increased competition or elevated moisture index. Long-term mortality increases were not driven by faster growth; instead, stand-level basal area increment either remained unchanged or declined across biomes. However, mortality was strongly associated with rising temperatures over time. These findings underscore an emerging vulnerability in ecosystems once considered resilient, raising concerns about the long-term sustainability of forest carbon sinks under future climate scenarios.

Research sample

This study combines and harmonizes 12 datasets to create the most extensive forest demographic record in Australia, covering a period of 83 years (1941–2023). It incorporates over 2,700 plots representing four major biomes: tropical savannas, tropical rainforests, warm temperate forests, and cool temperate forests. The dataset includes detailed information on 203,721 trees from 958 species, representing a wide range of geographical and ecological gradients.

Sampling strategy

Tree census data were collected from 2,724 plots across Australia, spanning 83 years (1941–2023). All trees with DBH \geq 5 cm or 10 cm were tagged, recorded, and remeasured at irregular time intervals.

Data collection

Plots were selected based on specific criteria to ensure data consistency: (1) Plots were at least 0.04 ha in size; (2) Trees with DBH \geq 5 cm were measured at least twice; (3) Plots with fire-induced mortality or complete tree loss were excluded to minimize disturbance effects; (4) Measurement intervals were at least one year to capture annual mortality trends; (5) Each plot contained at least 10 trees at the first census to reduce demographic variability; (6) Spatial coordinates were required to derive relevant climatic data.

Timing and spatial scale

The dataset covers forest plots distributed across Australia's major biomes over an 83-year period.

Data exclusions

We excluded trees that were logged during the census and omitted any census periods affected by bushfires to ensure the analysis focused on natural mortality patterns.

Reproducibility	<input type="text" value="This work is based on long-term monitoring rather than experiments."/>
Randomization	<input type="text" value="Not relevant"/>
Blinding	<input type="text" value="Not relevant"/>
Did the study involve field work?	<input checked="" type="checkbox"/> Yes <input type="checkbox"/> No

Field work, collection and transport

Field conditions	<input type="text" value="Our heterogeneous plots are shaped by distinct climate and disturbance regimes, resulting in distinct vegetation types. Tropical savannas experience strong seasonal rainfall and frequent fire events. Tropical rainforests, characterized by high moisture availability and dense canopies, are periodically impacted by tropical cyclones. Warm and cool temperate forests have moderate to high rainfall variability and are periodically affected by droughts and wildfires."/>
Location	<input type="text" value="This study included a heterogeneous sample of forest plots across Australia, encompassing tropical savannas, rainforests, and warm and cool temperate forests."/>
Access & import/export	<input type="text" value="Describe the efforts you have made to access habitats and to collect and import/export your samples in a responsible manner and in compliance with local, national and international laws, noting any permits that were obtained (give the name of the issuing authority, the date of issue, and any identifying information)."/>
Disturbance	<input type="text" value="Most plots, except in tropical rainforests, are managed and subject to logging."/>

Reporting for specific materials, systems and methods

We require information from authors about some types of materials, experimental systems and methods used in many studies. Here, indicate whether each material, system or method listed is relevant to your study. If you are not sure if a list item applies to your research, read the appropriate section before selecting a response.

Materials & experimental systems

n/a	Included in the study
<input checked="" type="checkbox"/>	<input type="checkbox"/> Antibodies
<input checked="" type="checkbox"/>	<input type="checkbox"/> Eukaryotic cell lines
<input checked="" type="checkbox"/>	<input type="checkbox"/> Palaeontology and archaeology
<input checked="" type="checkbox"/>	<input type="checkbox"/> Animals and other organisms
<input checked="" type="checkbox"/>	<input type="checkbox"/> Clinical data
<input checked="" type="checkbox"/>	<input type="checkbox"/> Dual use research of concern
<input checked="" type="checkbox"/>	<input type="checkbox"/> Plants

Methods

n/a	Included in the study
<input checked="" type="checkbox"/>	<input type="checkbox"/> ChIP-seq
<input checked="" type="checkbox"/>	<input type="checkbox"/> Flow cytometry
<input checked="" type="checkbox"/>	<input type="checkbox"/> MRI-based neuroimaging

Plants

Seed stocks	<input type="text" value="Report on the source of all seed stocks or other plant material used. If applicable, state the seed stock centre and catalogue number. If plant specimens were collected from the field, describe the collection location, date and sampling procedures."/>
Novel plant genotypes	<input type="text" value="Describe the methods by which all novel plant genotypes were produced. This includes those generated by transgenic approaches, gene editing, chemical/radiation-based mutagenesis and hybridization. For transgenic lines, describe the transformation method, the number of independent lines analyzed and the generation upon which experiments were performed. For gene-edited lines, describe the editor used, the endogenous sequence targeted for editing, the targeting guide RNA sequence (if applicable) and how the editor was applied."/>
Authentication	<input type="text" value="Describe any authentication procedures for each seed stock used or novel genotype generated. Describe any experiments used to assess the effect of a mutation and, where applicable, how potential secondary effects (e.g. second site T-DNA insertions, mosaicism, off-target gene editing) were examined."/>